Natural anomaly mediation from the landscape with implications for LHC SUSY searches

Howard Baer [1,*] Vernon Barger, [2,†] Jessica Bolich, [1,‡] Juhi Dutta [1,§] and Dibyashree Sengupta [3,∥]

[1] *Department of Physics and Astronomy, University of Oklahoma, Norman, Oklahoma 73019, USA*
[2] *Department of Physics, University of Wisconsin, Madison, Wisconsin 53706, USA*
[3] *INFN, Laboratori Nazionali di Frascati, Via E. Fermi 54, 00044 Frascati (RM), Italy*

(Received 5 December 2023; accepted 22 January 2024; published 15 February 2024)

Supersymmetric models with the anomaly-mediated supersymmetry (SUSY) breaking (AMSB) form for soft SUSY breaking terms arise in two different settings: (1) extra-dimensional models where SUSY breaking occurs in a sequestered sector, and (2) $4-d$ models with dynamical SUSY breaking in a hidden sector where scalars gain masses of order the gravitino mass $m_{3/2}$, but gaugino masses and trilinear soft terms are assumed to be of the AMSB form. Both models run into serious conflicts with (1) LHC sparticle and Higgs mass constraints, (2) constraints from winolike weakly interacting massive particle dark matter searches, and (3) bounds from naturalness. These conflicts may be avoided by introducing minor changes to the underlying phenomenological models consisting of nonuniversal bulk scalar Higgs masses and A terms, providing a setting for natural anomaly mediation (nAMSB). In nAMSB, the wino is still expected to be the lightest of the gauginos, but the Higgsinos are expected to be the lightest electroweakinos (EWinos) in accord with naturalness. We examine what sorts of spectra are expected to emerge when nAMSB arises from a string landscape setting: While model 2 can only be natural for a Higgs mass $m_h \lesssim 123$ GeV, model 1 can accommodate naturalness along with $m_h \sim 125$ GeV while still respecting LHC bounds on sparticle masses. We explore the LHC phenomenology of nAMSB models where we find that for Higgsino pair production, typically larger dilepton mass gaps arise from the soft dilepton-plus-jets signature than in models with gaugino mass unification. For wino-pair production, the higher $m_{3/2}$ portion of nAMSB parameter space is excluded by recent LHC bounds from gaugino pair production searches. We characterize the dominant LHC signatures arising from the remaining lower $m_{3/2} \sim 90$–200 TeV range of parameter space, which should be fully testable at high-luminosity LHC via EWino pair production searches.

DOI: 10.1103/PhysRevD.109.035011

I. INTRODUCTION

Supersymmetric models [1] based on anomaly-mediated supersymmetry (SUSY) breaking (AMSB) arose from two different setups.

A. AMSB0: (Giudice, Luty, Murayama, and Rattazzi)

The second, by Giudice *et al.* [2], which we label as *AMSB*0, was motivated by four-dimensional models where SUSY is broken dynamically in the hidden sector [3] and where SUSY breaking was communicated to the visible sector via gravity. The motivation here was that the SUSY breaking scale $m_{\rm hidden}$ might be generated nonperturbatively via gaugino condensation and would then be exponentially suppressed relative to the Planck scale via dimensional transmutation [4]: $m_{\rm hidden} \sim e^{-8\pi^2/g^2} m_P$, where m_P is the reduced Planck scale. This would not only stabilize the weak scale (via SUSY) but also explain its exponential suppression from the Planck scale: $m_{\rm weak} \sim m_{\rm soft} \sim m_{\rm hidden}^2/m_P$, where $m_{\rm hidden} \sim 10^{11}$ GeV. Now in gravity mediation, gaugino masses arise via

$$\int d^2\theta f_{AB}\left(\frac{S}{m_P}\right) W_\alpha^A W^{B\alpha} \tag{1}$$

with f_{AB} the gauge kinetic function depending on hidden sector fields S and where the F term of S acquires a SUSY breaking value F_S; the gaugino masses arise as $m_\lambda \sim (F_S/m_P) \sim m_{3/2} \sim m_{\rm soft} \sim m_{\rm weak}$. However, if no hidden

*baer@nhn.ou.edu
†barger@pheno.wisc.edu
‡Jessica.R.Bolich-1@ou.edu
§juhi.dutta@ou.edu
∥Dibyashree.Sengupta@lnf.infn.it

sector singlets are available as in (most) dynamical supersymmetry breaking models [5],[1] then the gaugino masses are expected instead at the keV scale, which would be experimentally excluded. However, Ref. [2] found that the one-loop renormalization of the visible sector gauge couplings is given by [7]

$$\frac{1}{4}\int d^2\theta\left(1-\frac{g^2 b_0}{16\pi^2}\log\frac{\Lambda^2}{\square}\right)W^\alpha W_\alpha + \text{H.c.}, \tag{2}$$

where b_0 is the coefficient of the relevant gauge group beta function and $\square$ is the d'Alembertian operator. This leads to SUSY breaking gaugino masses via replacement of the UV cutoff Λ by the spurion superfield $\Lambda \exp(m_{3/2}\theta^2)$ leading to (loop-suppressed) gaugino masses [8][2]

$$m_\lambda = -\frac{g^2 b_0}{16\pi^2} m_{3/2}. \tag{3}$$

For $m_{3/2} \sim 100$ TeV, $m_\lambda \sim 1$ TeV as required to gain $m_{\rm weak} \sim m_{W,Z,h} \sim 100$ GeV. Similarly, the trilinear soft (A) terms are not allowed at tree level if no singlets are available for a

$$\int d^2\theta \frac{S}{m_P}\phi_i\phi_j\phi_k \tag{4}$$

coupling (where the ϕ_i are generic visible sector superfields). The A terms can also arise at one-loop level in AMSB and are proportional to derivatives of the anomalous dimensions. Scalar masses, on the other hand, arise from

$$\int d^2\theta d^2\bar{\theta}\frac{S^\dagger S}{m_P^2}\phi^\dagger\phi, \tag{5}$$

and are not protected by symmetries, and so they can be much larger $m_\phi^2 \sim m_{3/2}^2$ and can gain their gravity-mediated form. This form of scalar mass generation suffers from the usual SUSY flavor problem that is endemic to gravity mediation.

The AMSB0 model thus yields a hierarchy of soft terms $m_\phi \gg m_\lambda \sim A$ as noted by Wells [13] in what he dubbed PeV SUSY [14]. This model also motivated realizations of split [15,16] and minisplit [17] SUSY models. These later models eschew the notion of naturalness in hopes of a landscape solution to the naturalness problem, thus allowing for scalar masses in the range of 100–1000 TeV (for minisplit) and ranging up to $m_\phi \sim 10^9$ TeV for split SUSY. Split SUSY predicts a light Higgs mass $m_h \sim$ 130–160 GeV [18]. The discovery of a Standard-Model-(SM) like Higgs boson with mass $m_h \sim 125$ GeV motivated a retreat to scalars in the range of minisplit models which allow for $m_h \sim 125$ GeV along with small A terms. A value of $m_h \simeq 125$ GeV can also be realized by TeV-scale top squarks but with near maximal stop mixing from large A terms [19,20].

Since scalar masses arise as in gravity mediation, this *AMSB*0 model may still be plagued by flavor problems, although these may be softened by the rather large values of scalar masses which are expected: a (partial) decoupling solution to the SUSY flavor problem [21]. It also gave rise to unique phenomenological signatures [22] since in AMSB the wino rather than the bino was expected to be the lightest SUSY particle (LSP).

B. AMSB (RS)

Alternatively, in the Randall-Sundrum (RS) AMSB model [23] (*AMSB*), it was posited that SUSY breaking arose in a hidden sector sequestered from the visible sector in extra-dimensional spacetime. In such a setup, the leading contribution to all soft SUSY breaking terms was from the superconformal anomaly and suppressed by a loop factor from the gravitino mass $m_{3/2}$. In this form of AMSB, a common value of scalar masses was expected, thus avoiding the SUSY flavor problem which seems endemic to models of gravity mediation. Also, since $m_{\rm soft} \ll m_{3/2}$, the cosmological gravitino problem could be avoided since in the early Universe thermally produced gravitinos could decay before the onset of big bang nucleosynthesis [24]. In both cases of *AMSB* and *AMSB*0, the thermally underproduced winolike weakly interacting massive particles (WIMPs) could have their relic abundance nonthermally enhanced by either gravitino [25] or moduli-field decays [26,27]. A drawback in the case of *AMSB* was that soft slepton masses were derived to be tachyonic, thus leading to charge-breaking vacua in the scalar potential. Some extra contributions to scalar masses arising from fields propagating in the bulk of spacetime could be postulated to avoid this problem [23].

C. Further deliberations on AMSB

Some further notable theoretical explorations of AMSB soft terms include Gaillard *et al.* [28] where AMSB soft terms arose as quantum corrections under Pauli-Villars regularization of supergravity. In Anisimov *et al.* [29,30], brane world SUSY breaking (as in the RS model) was examined, and it was found to be insufficient to guarantee the needed sequestering between hidden and observable sectors to generate dominant AMSB soft terms and flavor-conserving scalar masses. In Ref. [31], Luty presents pedagogical lectures on SUSY breaking leading up to and including AMSB. In Ref. [32], the connection of AMSB with dimensional transmutation is examined as a solution to the tachyonic slepton problem. In Ref. [33], Dine and Seiberg (DS) clarify the derivation of AMSB soft terms and relate them to the gaugino counterterm. In Ref. [34], de Alwis presents the derivation of AMSB soft

[1]For an exception, see, e.g., [6].
[2]The AMSB contributions to gaugino masses were already presaged by Refs. [9–12].

terms and emphasizes their origin in work by Kaplunovsky and Louis [12] and DS, and shows there may be additional soft term contributions. This inspires his later development of the gaugino AMSB model [35]. In Ref. [36], a clarifying derivation of AMSB soft terms is presented. In Ref. [37], Sanford and Shirman develop an arbitrary conformal compensator formalism, which allows extrapolation between RS and DS derivations. In Ref. [38], anomaly mediation from IIB string theories is examined. In Ref. [39], the AMSB connection with gravitino mediation vs Kähler mediation is examined. This work is extended to scalar masses in Ref. [40]. In Ref. [41], Dine and Draper examine anomaly mediation in local effective theories. In Ref. [42], de Alwis examines the interplay of AMSB with spontaneous SUSY breaking. In Ref. [43], the connection between AMSB gaugino masses and the path integral measure is examined.

An alternative route to models with AMSB soft terms was developed by Luty and Sundrum [44] in models with strong hidden sector conformal dynamics. In these $4-d$ models, strong hidden sector conformal dynamics leads to a suppression, or sequestering, of usual soft terms due to higher-dimensional operators which mix the hidden and visible sectors. The suppression of gravity-mediated soft terms occurs between the messenger scale (taken here to be m_P) and some intermediate scale $m_{\rm int}$ where conformal symmetry becomes broken. In such a case, the loop-suppressed AMSB soft terms may become dominant. In Ref. [45], the conformal suppression acts upon scalar masses and the $B\mu$ term, but in Refs. [46,47], it is emphasized that conformal sequestering may also act on the gaugino sector.

D. Status of the minimal phenomenological AMSB model (mAMSB)

A minimal phenomenological AMSB model (mAMSB) was proposed in Refs. [48,49] with parameter space

$$m_0, \quad m_{3/2}, \quad \tan\beta, \quad \mathrm{sign}(\mu) \quad (mAMSB), \tag{6}$$

where m_0 was an added universal bulk scalar mass, and the gravitino mass $m_{3/2}$ set the scale for the AMSB soft terms $m_{\rm AMSB} \sim c(g^2/16\pi^2)m_{3/2}$ with c a calculable constant of order unity and g is a gauge group coupling constant. The bulk scalar mass is generic to the *AMSB*0 setup and phenomenologically required to gain positive slepton squared masses in *AMSB*. Various studies of mAMSB at LHC appeared in Refs. [50–54].

At present, both of these setups within the mAMSB model seem phenomenologically disfavored and perhaps even ruled out. The first problem is that in mAMSB the SUSY conserving μ parameter is typically fine-tuned to large values compared to the measured value of the weak scale $m_{\rm weak} \sim m_{W,Z,h} \sim 100$ GeV, thus violating [55] even the most conservative measure of naturalness $\Delta_{\rm EW}$ [56,57], where $\Delta_{\rm EW}$ is defined as the largest value on the right-hand side (rhs) of the scalar potential minimization condition

$$m_Z^2/2 = \frac{m_{H_d}^2 + \Sigma_d^d - (m_{H_u}^2 + \Sigma_u^u)\tan^2\beta}{\tan^2\beta - 1} - \mu^2 \tag{7}$$

divided by $m_Z^2/2$. The second problem is that the small values of mAMSB A terms typically lead to too small a value of $m_h \ll 125$ GeV unless third-generation soft scalar masses lie in the 10–100 TeV range [58,59], thus also violating naturalness [55] via the radiative corrections $\Sigma_u^u(\tilde{t}_{1,2})$, leading again to a large value for the electroweak fine-tuning measure $\Delta_{\rm EW}$. A third problem is that wino-only dark matter [26] now seems excluded by a combination of direct and indirect WIMP search experiments [60–62]. This latter exclusion may be circumvented in cases of mixed axion-wino dark matter (DM) (two DM particles) wherein the relic wino abundance forms only a small portion of the total DM abundance [63]. This latter scenario posits a Peccei-Quinn axion which also solves the fine-tuning problem of the θ parameter in the QCD sector.

E. Natural anomaly-mediated SUSY breaking (nAMSB)

In Ref. [64], two minor changes to the mAMSB model were suggested to circumvent its undesirable phenomenological properties.[3] First, separate bulk masses for $m_{H_u} \neq m_{H_d} \neq m_0$ were applied to scalar masses, which then allowed for a small μ parameter in accord with naturalness [a unified mass m_0 just for matter scalars is highly motivated by the fact that the matter superfields are unified within the 16-dimensional spinor rep of $SO(10)$]. Second, bulk contributions to trilinear soft terms A_0 were advocated, which then allowed for large stop mixing which in turn uplifts the Higgs mass $m_h \to \sim 125$ GeV [65] without requiring the stop sector to lie in the unnatural multi-TeV range or beyond. These two adjustments allowed for EW naturalness and for $m_h \sim 125$ GeV. Models with these attributes were denoted as natural AMSB (nAMSB):

$$m_0(i), \quad m_{H_u}, \quad m_{H_d}, \quad m_{3/2}, \quad A_0, \quad \tan\beta \quad (nAMSB'), \tag{8}$$

where we also allow for possible nonuniversal bulk contributions to the different generations $i = 1$–3. It is convenient to then trade the high-scale parameters $m_{H_u}^2$ and $m_{H_d}^2$ for weak-scale parameters μ and m_A using the scalar potential minimization conditions [66,67].

Like mAMSB, the nAMSB model has winos as the lightest of the gauginos. Unlike mAMSB, the nAMSB model (usually) has Higgsinos as the lightest EWinos, in

[3]These "changes" were actually suggested as default parameters in the original RS paper Ref. [23].

accord with naturalness. By requiring the natural axionic solution to the strong CP problem, one then expects mixed axion plus Higgsino-like WIMP dark matter [68,69], and one can circumvent the constraints on wino-only dark matter [62].

F. nAMSB from the landscape

The advent of the string theory landscape [70,71] led to some major changes in SUSY models with AMSB soft terms. First, it was found that flux compactification [72] of type-IIB string models on Calabi-Yao orientifolds led to enormous numbers of string vacuum states (10^{500} is a prominently quoted number [73,74], although much larger numbers have also been found in F-theory compactifications [75]). Such large numbers of vacuum possibilities allow for Weinberg's [76] anthropic solution to the cosmological constant (CC) problem and "explains" the fine-tuning of Λ_{CC} to a part in 10^{120}. Then, if the CC is fine-tuned by anthropics, might one also allow for the little hierarchy $m_{\rm weak} \ll m_{\rm soft}$ to also be fine-tuned? In split SUSY, electroweak naturalness is eschewed, while WIMP dark matter and gauge coupling unification are retained [13,15,77]. A possible model framework for split SUSY would then be charged SUSY breaking [14,16], wherein tree level gaugino masses (and A terms) are forbidden by some symmetry (perhaps R symmetry?), while scalar masses are allowed as heavy as one likes. Values of $m_{\rm scalar} \sim 10^9$ GeV were entertained, leading to a signature of long-lived gluinos. The heavy scalars also allowed for a decoupling solution to the SUSY flavor and CP problems [21]. In split SUSY, one expects light Higgs masses in the $m_h \sim 130$–160 GeV range [18,78], in contrast to the 2012 Higgs discovery with $m_h \simeq 125$ GeV. To accommodate the measured Higgs mass, scalar masses were dialed down to the 10^3 TeV range. These minisplit models [17,79] then allowed for $m_h \sim 125$ GeV while still potentially allowing for a decoupling solution to the SUSY flavor and CP problems. However, only recently has the occurrence frequency of highly fine-tuned SUSY models been examined in an actual landscape context. In Ref. [80], a toy model of the landscape was developed, and it was shown that EW natural models should be more likely than fine-tuned models to emerge from a generic landscape construction. In retrospect, the reason is rather simple. In Agrawal *et al.* [81] (ABDS), it was found that within a multiverse wherein each pocket universe would have a different value for its weak scale, only complex nuclei, and hence, complex atoms (which seem necessary for life as we know it), would arise if the pocket-universe value of the weak scale were within a factor of a few of its measured value in our Universe (OU): $0.5 m_{\rm weak}^{OU} \lesssim m_{\rm weak}^{PU} \lesssim 5 m_{\rm weak}^{OU}$. We call this range of $m_{\rm weak}^{PU}$ the ABDS window. Now in models where all contributions to the weak scale [to the rhs of Eq. (7)] are natural (in that they lie within the ABDS window), the remaining parameter selection [typically, either $\mu(\rm weak)$ or $m_{H_u}(\rm weak)$] will also have a wide range of possibilities, all lying within the ABDS window, to gain an ultimate value for $m_{\rm weak}$ within the ABDS window. On the other hand, if any contribution to $m_{\rm weak}$ is far beyond $m_{\rm weak}$, then fine-tuning is needed, and only a tiny portion of parameter space will lead to $m_{\rm weak} \sim 100$ GeV. This scheme was then used in Ref. [82] to compute relative probabilities P_μ for different natural and fine-tuned SUSY models (and the SM) to emerge from the landscape. For instance, from Ref. [82], it was found that for a radiative natural SUSY model, where all contributions to the weak scale lie within the ABDS window, a relative probability $P_\mu \sim 1.4$ was computed, while the SM, valid up to the reduced Planck mass m_P, had $P_\mu \sim 10^{-26}$. Also, split SUSY—with scalar masses at 10^6 TeV—had $P_\mu \sim 10^{-11}$. Other models such as CMSSM [83], PeV SUSY [14], spread SUSY [84], minisplit [17], high-scale SUSY [85], and G_2MSSM [86] were also examined and found to have tiny values of P_μ. Thus, while the emergence of EW fine-tuned models is logically possible from the landscape, their likelihood is highly suppressed compared to natural models: Natural SUSY models are much more plausible as a low energy effective field theory (LE EFT) realization of the string landscape.

With the above considerations in mind, in this paper we first wish to explore in Sec. II the expectations for Higgs boson and sparticle masses from the nAMSB model with sequestered sector SUSY breaking, as might be expected from SUSY brane-world models, and as characterized by the presence of bulk A terms ($A_0 \neq 0$ but also including AMSB A terms). The nAMSB0 model with $A_0 = 0$ has been shown in Fig. 2 of Ref. [64] to allow for naturalness ($\Delta_{\rm EW} \lesssim 30$) but only if $m_h \lesssim 123$ GeV. With the string landscape in mind, we expect the various bulk soft terms and $m_{3/2}$ to be distributed as a power-law draw

$$P_{\rm soft} \sim m_{\rm soft}^n \tag{9}$$

to large values in the multiverse as suggested by Douglas [87]. By combining the draw to large soft terms with the requirement of a weak scale within the ABDS window, the putative distribution of Higgs and sparticle masses from the landscape may be derived in the context of those string models which reduce to an nAMSB low energy effective theory. Generically, under charged SUSY breaking with gravity-mediated scalar masses, we expect nonuniversality within different grand unified theory multiplets and different generations, so we adopt independent masses $m_0(i)$, ($i = 1$–3 a generation index), along with $m_{H_u} \neq m_{H_d}$. Motivated by the fact that all members of each generation fill out a complete 16D spinor of $SO(10)$, we maintain universality within each generation (as emphasized by Nilles *et al.* [88]). One issue is that the bulk trilinear soft terms A_0 are expected to be forbidden under charged SUSY breaking [14]. These results show the difficulty of deriving

$m_h \sim 125$ GeV in such models without bulk A terms. Thus, our ultimate parameter space is

$$m_0(i),\quad m_{3/2},\quad A_0,\quad \mu,\quad m_A,\quad \tan\beta \quad (nAMSB). \tag{10}$$

We then restrict ourselves to a set of string landscape vacua with the minimal supersymmetric Standard Model as the low energy EFT, but where gauginos gain AMSB masses, but the remaining soft terms scan within the multiverse and include bulk terms. (While soft terms are expected to be correlated within our Universe, they may scan within the multiverse [89].)

With this setup in mind, the remainder of this paper is organized as follows. In Sec. II, we assume a simple $n = +1$ power-law draw [as in Eq. (9)] on soft terms in the landscape, and plot out probability functions for the various expected Higgs and sparticle masses for *nAMSB* with $A_0 \neq 0$. These models can be natural while also respecting $m_h \sim 125$ GeV. In Sec. III, we present several *AMSB* benchmark points and model lines. In Sec. IV, we present sparticle production cross sections expected from nAMSB along our given model line. Here, we find that typically Higgsino and wino-pair production is dominant over the entire range of $m_{3/2}$ values. In Sec. V, we discuss the wino decays in nAMSB for the dominantly produced sparticles. In Sec. VI, we discuss the main signal channels expected for LHC searches for nAMSB. Given the AMSB weak-scale gaugino mass ratio $M_1 : M_2 : M_3 \sim 3:1:8$, it is possible that strong new limits on gaugino pair production from the LHC could exclude *nAMSB* up to and perhaps even beyond its naturalness limit. However, there remains a low mass window with $m(\text{wino}) \gtrsim m(\text{Higgsinos})$ which is still allowed due to the semicompressed spectrum of the EWinos. After implementing present LHC constraints on nAMSB parameter space, in Sec. VII we discuss the most favorable avenues for future SUSY searches within the nAMSB framework: via Higgsino and wino-pair production. Our summary and conclusions follow in Sec. VIII.

II. SPARTICLE AND HIGGS MASSES IN *nAMSB* FROM THE LANDSCAPE

Here, we scan over parameters with a landscape-motivated $P_{\text{soft}} \sim m^1_{\text{soft}}$ (linear) draw to large soft terms [87,90]:

(i) $m_{3/2}$: 80–400 TeV,
(ii) $m_0(1,2)$: 1–20 TeV,
(iii) $m_0(3)$: 1–10 TeV,
(iv) A_0: 0–± 20 TeV,
(v) m_A: 0.25–10 TeV, and
(vi) $\tan\beta$: $3-60$ (flat scan).

In accord with naturalness, we fix $\mu = 250$ GeV. In lieu of requiring the pocket-universe value of m_Z^{PU} to lie within the ABDS window, we instead invoke $\Delta_{\text{EW}} < 30$ to avoid fine-tuning from terms beyond the ABDS window: The fine-tuned solutions are much more rare compared to non-fine-tuned (natural) solutions because in the fine-tuned case, the scan parameter space rapidly shrinks to a tiny interval [80,82]. For the present case, we restrict the landscape to those vacuum solutions which lead to the nAMSB model as the low energy effective field theory, but where the contributions to the soft breaking terms scan over this restricted portion of the multiverse.

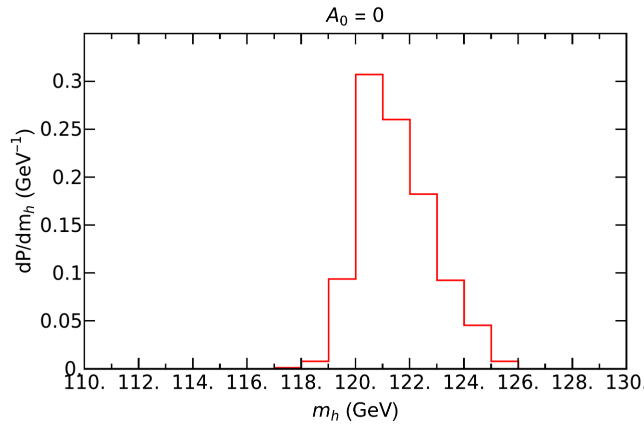

FIG. 1. Plot of dP/dm_h from an $n = 1$ landscape scan in the nAMSB0 model where $A_0 = 0$.

Our first results are shown in Fig. 1 for the nAMSB0 model where A_0 is fixed at zero. In this case, we see that the probability distribution peaks at $m_h \sim 120$ GeV and falls sharply with increasing m_h. While some probability still exists for $m_h \sim 125$ GeV, we henceforth move beyond nAMSB0 to the nAMSB model with $A_0 \neq 0$ where prospects for generating a Higgs mass m_h in accord with LHC data are much better.

Our first results for nAMSB are shown in Fig. 2. In Fig. 2(a), we show the differential probability distribution dP/dm_h vs m_h, where P is the probability normalized to unity. The red histogram shows the full probability distribution while the blue-dashed histogram shows the same distribution after LHC sparticle mass limits (discussed in Sec. VI) are imposed. We see that dP/dm_h has only small values for $m_h \lesssim 123$ GeV, but then peaks sharply in the range $m_h \sim 125$–127 GeV. This is in accord with similar results in models with unified gaugino masses [90] or mirage-mediated[4] gaugino masses [94]: Basically, the soft terms $m_0(1,2)$, $m_0(3)$, A_0, m_A, and $m_{3/2}$ are selected to be as large as possible subject to the condition that the derived

[4]The mirage-mediated (MM) SUSY breaking model derives comparable moduli- and anomaly-mediated contributions to soft SUSY breaking terms [91,92] in the context of string flux compactifications. The term mirage refers to the fact that in MM the three gaugino masses unify at an intermediate mass scale whose value depends on the relative moduli- versus anomaly-mediated contributions to gaugino masses. While the original formulation of MM seemed in conflict with naturalness and a Higgs mass $m_h \simeq 125$ GeV [55], the MM model was generalized from discrete to continuous variations in soft terms, which then allowed for $m_h = 125$ GeV while maintaining naturalness [93].

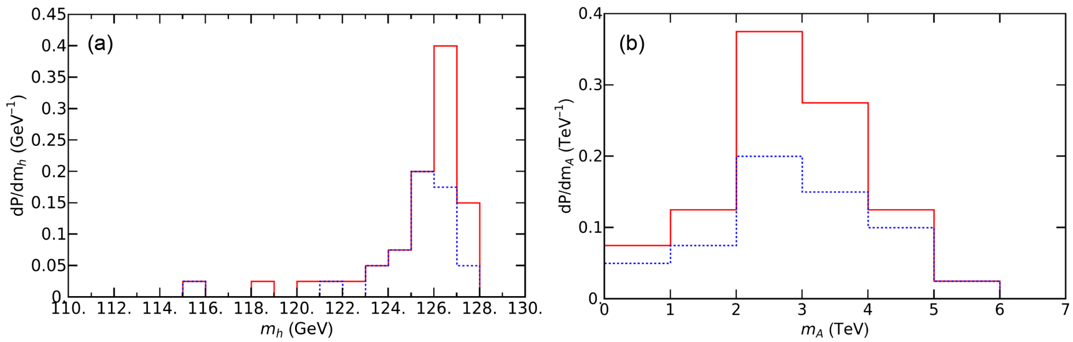

FIG. 2. Plot of (a) dP/dm_h and (b) dP/dm_A from an $n = 1$ landscape scan in the nAMSB model. The red histogram shows the full probability distribution, while the blue-dashed histogram shows the remaining distribution after LHC sparticle mass limits are imposed.

value of m_Z^{PU} lies within the ABDS window. This pulls the top-squark soft terms $m_0(3)$ large into the ~5 TeV range (but not too large) and also the bulk term A_0 to large—nearly maximal—mixing values, but not so large as to lead to charge and/or color breaking (CCB) minima of the scalar potential (CCB or no-electroweak-symmetry-breaking minima must be vetoed as not leading to a livable universe as we know it). These conditions pull m_h up to the vicinity of ~125 GeV. We also show in Fig. 2(b) the distribution in pseudoscalar Higgs mass m_A, where m_A contributes directly to the weak scale through Eq. (7) since for $m_{H_d} \gg m_Z$, $m_A \simeq m_{H_d}$ (and $m_H \sim m_{H^\pm} \sim m_A$). Here, we see that m_A reaches peak probability around ~2.5 TeV, somewhat beyond the reach of the high-luminosity (HL) LHC [95]. Maximally, m_A can extend up to ~6 TeV before overcontributing to the weak scale.

In Fig. 3, we show the probability for selected nAMSB model input parameters. In Fig. 3(a), the distribution $dP/dm_{3/2}$ rises to a broad peak between $m_{3/2}$: 100 and 250 TeV and cuts off sharply around 300 TeV. The upper cutoff on $m_{3/2}$ occurs because as $m_{3/2} \to 300$ TeV, then $m_{\tilde{g}}$ is pulled beyond 5–6 TeV. In this case, the coupled renormalization group equations pull stop masses so high that $\Sigma_u^u(\tilde{t}_{1,2})$ starts contributing too much to the weak scale. In Fig. 3(b), we show the distribution in first-/second-generation sfermion soft mass $m_0(1,2)$. Here, the distribution rises steadily to the scan upper limit since first-/second-generation sfermion contributions to the weak

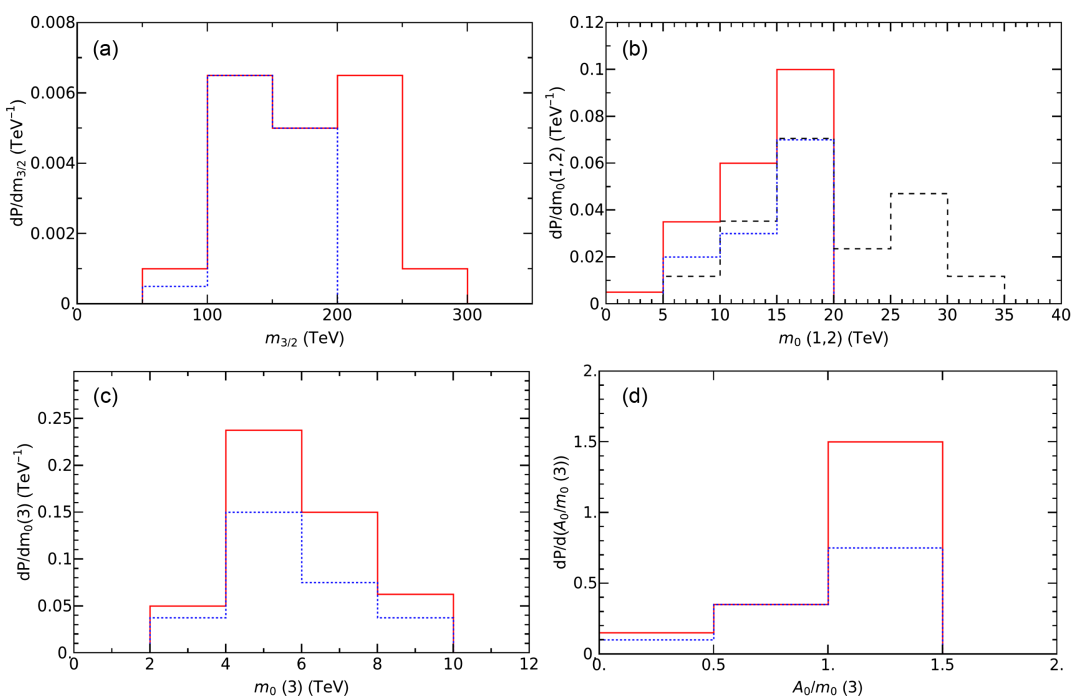

FIG. 3. Plot of (a) $dP/dm_{3/2}$, (b) $dP/dm_0(1,2)$, (c) $dP/dm_0(3)$, and (d) $dP/d(A_0/m_0(3))$ from an $n = 1$ landscape scan in the nAMSB model. The red histogram shows the full probability distribution, while the blue-dashed histogram shows the remaining distribution after LHC sparticle mass limits are imposed.

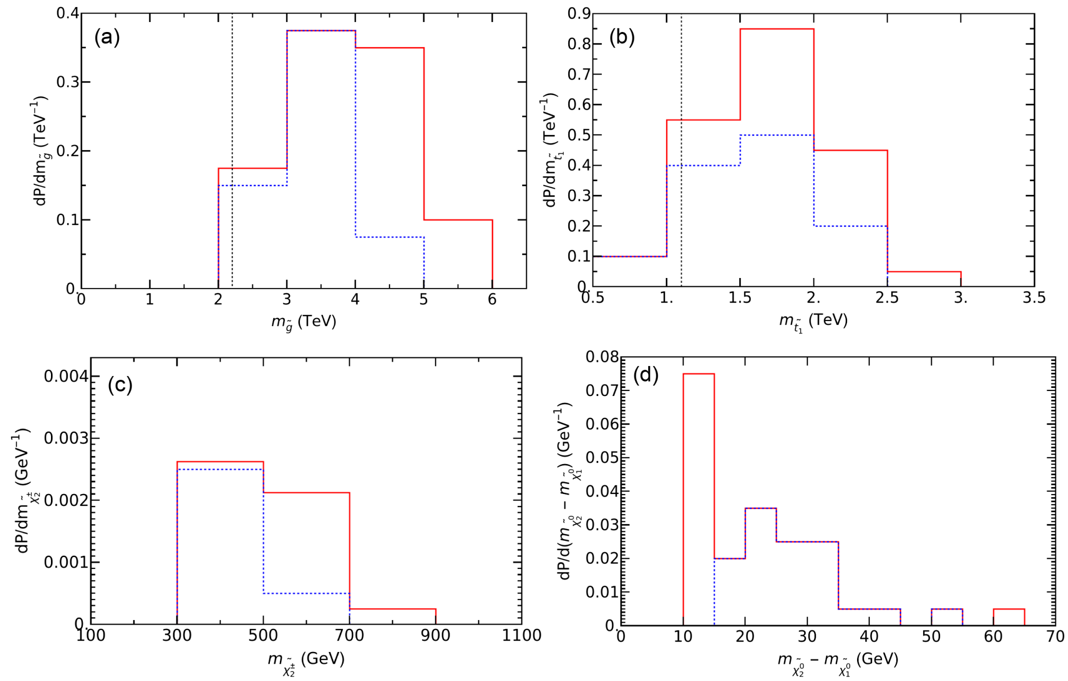

FIG. 4. Plot of (a) $dP/dm_{\tilde g}$, (b) $dP/dm_{\tilde t_1}$, (c) $dP/dm_{\tilde\chi_2^\pm}$, and (d) $dP/d(m_{\tilde\chi_2^0} - m_{\tilde\chi_1^0})$ from an $n = 1$ landscape scan in the nAMSB model. The red histogram shows the full probability distribution, while the blue-dashed histogram shows the remaining distribution after LHC sparticle mass limits are imposed.

scale $\Sigma_u^u(\tilde f_{1,2})$ are proportional to the corresponding fermion Yukawa coupling. This pull to multi-TeV values of first-/second-generation squarks and sleptons provide a landscape amelioration of the SUSY flavor and *CP* problems [96]. We also show as a black-dashed histogram the results from a special run with increased upper scan limit of $m_0(1,2) < 50$ TeV. In this case, the distribution peaks at $m_0(1,2) \sim 15$–30 TeV before getting damped by the anthropic condition that m_Z^{PU} lies within the ABDS window. In Fig. 3(c), we show the distribution in third-generation soft term $m_0(3)$. In this case, the distribution peaks at ∼5 TeV albeit with a distribution extending between 2 and 10 TeV. The reason for the upper cutoff is usually that the $\Sigma_u^u(\tilde t_{1,2})$ contribution to the weak scale becomes too large. Finally, in Fig. 3(d), we show the distribution in the ratio $A_0/m_0(3)$. This distribution shows the prediction of large bulk A terms which actually suppress the contributions of $\Sigma_u^u(\tilde t_{1,2})$ to the weak scale [56]. But if A_0 gets too big, then one is pulled into CCB vacua [97], which fail the anthropic criteria.

In Fig. 4, we show the $n = +1$ landscape probability distribution predictions for various sparticle masses. In Fig. 4(a), we show the distribution in gluino mass $m_{\tilde g}$. The distribution begins around $m_{\tilde g} \sim 2$ TeV and peaks at $m_{\tilde g} \sim 3$–4.5 TeV. This "stringy natural" [98] distribution can explain why it was likely that the LHC would not discover weak-scale SUSY via gluino pair production at Run 2, and why gluino pair searches may even elude HL-LHC searches [99]. The light stop mass distribution is shown in Fig. 4(b) and predicts $m_{\tilde t_1} \sim 1$–2.5 TeV, which is mostly within range of the HL LHC [100]. In Fig. 4(c), we show the distribution in $m_{\tilde\chi_2^\pm}$ which is approximately the wino mass. Here, the bulk of the probability distribution lies between $M_2 \sim 300$ and 700 GeV, making wino-pair production an inviting target for LHC searches. In Fig. 4(d), we show the distribution in mass difference of the two lightest neutralinos: $m_{\tilde\chi_2^0} - m_{\tilde\chi_1^0}$. This mass gap is relevant for the reaction $pp \to \tilde\chi_1^0\tilde\chi_2^0$ where $\tilde\chi_2^0 \to f\bar f\tilde\chi_1^0$ and thus provides a kinematic upper bound for the $m(f\bar f)$ invariant mass. From the distribution, the mass gap peaks between 10 and 15 GeV with a tail extending out to 40 GeV (and even beyond).

III. *AMSB* BENCHMARK POINTS AND MODEL LINES

In this section, we compile three AMSB model benchmark points using the ISAJET 7.91 code [101] for sparticle and Higgs mass spectra. The 7.91 version includes several fixes which give better convergence in the nAMSB model than previous versions.

A. *mAMSB*, *nAMSB*0, and *nAMSB* benchmark points

1. *mAMSB benchmark*

In Table I, we list three AMSB model benchmark points from three different AMSB models but with similar underlying parameters which are convenient for comparison.

TABLE I. Input parameters and masses in GeV units for the mAMSB, nAMSB0, and nAMSB natural generalized anomaly-mediated SUSY benchmark points with $m_t = 173.2$ GeV using ISAJET 7.91.

Parameter	mAMSB	nAMSB0	nAMSB
$m_{3/2}$	125000	125000	125000
$\tan\beta$	10	10	10
$m_0(1,2)$	5000	10000	10000
$m_0(3)$	5000	5000	5000
A_0	0	0	6000
μ	1718.8	250	250
m_A	5185.3	2000	2000
$m_{\tilde{g}}$	2728.1	2803.0	2802.4
$m_{\tilde{u}_L}$	5460.8	10211.8	10210.9
$m_{\tilde{u}_R}$	5484.4	10289.0	10312.1
$m_{\tilde{e}_R}$	4965.1	9918.6	9889.4
$m_{\tilde{t}_1}$	3428.4	3165.3	1487.9
$m_{\tilde{t}_2}$	4564.6	4253.6	3657.9
$m_{\tilde{b}_1}$	4545.6	4238.5	3691.4
$m_{\tilde{b}_2}$	5435.8	5239.3	5165.7
$m_{\tilde{\tau}_1}$	4918.6	4789.1	4692.3
$m_{\tilde{\tau}_2}$	4945.1	4253.6	4978.0
$m_{\tilde{\nu}_\tau}$	4945.7	4940.9	4956.6
$m_{\tilde{\chi}_2^\pm}$	1746.6	393.6	387.9
$m_{\tilde{\chi}_1^\pm}$	366.2	241.2	238.1
$m_{\tilde{\chi}_4^0}$	1745.2	1176.6	1174.2
$m_{\tilde{\chi}_3^0}$	1742.4	402.4	395.0
$m_{\tilde{\chi}_2^0}$	1163.0	260.9	260.4
$m_{\tilde{\chi}_1^0}$	366.0	229.4	226.3
m_h	120.3	120.7	125.0
$\Omega_{\tilde{\chi}_1^0}^{TP}h^2$	0.009	0.01	0.01
$BF(b\to s\gamma)\times 10^4$	3.1	3.2	3.3
$BF(B_s\to\mu^+\mu^-)\times 10^9$	3.8	3.8	3.8
$\sigma^{SI}(\tilde{\chi}_1^0, p)$ (pb)	7.5×10^{-11}	1.8×10^{-8}	1.6×10^{-8}
$\sigma^{SD}(\tilde{\chi}_1^0 p)$ (pb)	1.7×10^{-7}	2.2×10^{-4}	2.6×10^{-4}
$\langle\sigma v\rangle\vert_{v\to 0}$ (cm^3/sec)	6.1×10^{-25}	2.4×10^{-25}	2.6×10^{-25}
$\Delta_{\rm EW}$	711	60	15.0

In column 2, we list sparticle and Higgs masses for the usual minimal AMSB model [48,49] where universal bulk scalar contributions m_0^2 were added to all AMSB scalar soft masses but no bulk A_0 terms were included. We take $m_{3/2} = 125$ TeV and $\tan\beta = 10$ with $m_0 = 5$ TeV. The μ term is fine-tuned to a value $\mu = 1719$ GeV to ensure $m_Z = 91.2$ GeV, so the model will be highly fine-tuned with $\Delta_{\rm EW} = 711$ (as listed). The gluino mass $m_{\tilde{g}} = 2.73$ TeV so that gluinos are safely beyond LHC Run 2 search limits which require $m_{\tilde{g}} \gtrsim 2.3$ TeV (in simplified models). The light Higgs mass $m_h = 120.3$ GeV: too light compared to its measured value (and so this benchmark point is ruled out). The LSP is winolike with mass $m_{\tilde{\chi}_1^0} = 366$ GeV, while $\tilde{\chi}_2^0$ is binolike and the $\tilde{\chi}_{3,4}^0$ and $\tilde{\chi}_2^\pm$ are Higgsino-like with mass $\sim\mu$. The top squark is not very mixed with $m_{\tilde{t}_1} = 3.43$ TeV, safely above LHC stop search limits. With a winolike LSP, the thermally produced relic abundance $\Omega_{\tilde{\chi}}^{TP}h^2 = 0.009$, underabundant by a factor ~ 13. Thus, nonthermal wino production mechanisms would need to be active to fulfill the relic abundance with pure wino dark matter, which would then be ruled out by indirect WIMP detection experiments, where winos could annihilate strongly in dwarf galaxies, thus yielding high energy gamma rays in violation of limits [62] from Fermi-LAT and HESS. Alternatively, a tiny abundance of wino DM could be allowed if some other particle such as axions constituted the bulk of dark matter [63].

2. nAMSB0 benchmark

Benchmark point nAMSB0 shows the expected sparticle and Higgs mass spectra from the generalized AMSB model inspired by dynamical supersymmetry breaking where hidden sector singlets are not allowed. This leads to allowed—but nonuniversal—scalar masses, while gaugino masses and A terms are suppressed and thus assume their loop-suppressed AMSB form. Thus, for nAMSB0 we adopt the parameter space Eq. (10) but with $A_0 = 0$. We adopt a natural value of $\mu = 250$ GeV with $m_A = 2$ TeV and also allow for higher first-/second-generation scalar masses, as expected from the landscape, with $m_0(1,2) = 10$ TeV, while $m_0(3) = 5$ TeV as in the mAMSB benchmark point.

For nAMSB0, the natural value of $\mu = 250$ GeV implies light Higgsinos so that while winos are still the lightest gauginos, the Higgsinos are the lightest EWinos, and thus the expected phenomenology markedly changes from mAMSB. The small value of μ also makes the nAMSB0 model much more natural than mAMSB, where $\Delta_{\rm EW}$ has dropped to 60. The dominant contributions to $\Delta_{\rm EW}$ come now from $\Sigma_u^u(\tilde{t}_{1,2})$. But the model is still somewhat unnatural since the largest contribution to the rhs of Eq. (7) is still ~ 500 GeV, outside the ABDS window [81], and thus in need of fine-tuning. Another problem is the light Higgs mass $m_h = 120.7$ GeV. Both of these issues arise from the rather small AMSB0 value for the trilinear soft terms.

3. nAMSB benchmark

In the fourth column of Table I, we list the nAMSB benchmark point which could arise from the sequestered SUSY breaking scenario of RS [23], where in addition to bulk scalar masses, bulk A terms are also expected. Here, we use the same parameters as in nAMSB0, except now we also allow $A_0 = 6$ TeV. The large trilinear soft term leads to large stop mixing which feeds into the m_h value (which is maximal for stop mixing parameter $x_t \sim \sqrt{6}m_{\tilde{t}}$) so that now the value of m_h is lifted to 125 GeV in accord with LHC measurements. Also, the large positive A term leads to cancellations in both of $\Sigma_u^u(\tilde{t}_1)$ and $\Sigma_u^u(\tilde{t}_2)$ leading to increased naturalness where now $\Delta_{\rm EW} = 15$. For the nAMSB0 benchmark, the more-mixed lighter stop mass has dropped to just $m_{\tilde{t}_1} \sim 1.5$ TeV, within striking distance of the HL LHC [100].

B. Corresponding AMSB model lines

In this subsection, we elevate each of the AMSB benchmark points to AMSB model lines where we keep the auxiliary parameters fixed as before but now allow the fundamental AMSB parameter $m_{3/2}$ to vary. We compute the AMSB model line spectra using Isasugra.

In Fig. 5, we first show the naturalness measure $\Delta_{\rm EW}$ for each model line. For the mAMSB model line, we see that $\Delta_{\rm EW}$ starts at ~100 for low $m_{3/2} \sim 50$ TeV, and then steadily increases to $\Delta_{\rm EW} \sim 10^4$ for $m_{3/2} \sim 500$ TeV. As for the mAMSB benchmark point, the dominant contribution to $\Delta_{\rm EW}$ comes from the (fine-tuned) μ parameter. This model line thus seems highly implausible for all $m_{3/2}$ values based on naturalness. We also show the nAMSB0 model line as the orange curve. Here, $\Delta_{\rm EW}$ ranges from 50 to 200 as $m_{3/2}$ varies over 50–500 TeV. While more natural than mAMSB, it still lies outside the ABDS window which is typified by $\Delta_{\rm EW} \lesssim 30$. The blue curve shows the nAMSB model line. In this case, $\Delta_{\rm EW}$ ranges from ~15 to 150. The line $\Delta_{\rm EW} = 30$ is shown by the dashed red curve. Here, we see the model line starts becoming unnatural for $m_{3/2} \gtrsim 265$ TeV.

In Fig. 6, we show the computed value of m_h along the three model lines. The LHC measured window is between m_h: 123 and 127 allowing for a ± 2 GeV theory error in the computed value of m_h. We see that the mAMSB model line enters the allowed region of m_h only for $m_{3/2} \gtrsim 400$ TeV, while the nAMSB0 model line enters the allowed m_h range for $m_{3/2} \gtrsim 300$ TeV. Both model lines are highly unnatural for such large $m_{3/2}$ values. However, the nAMSB model line is within the $m_h = 125 \pm 2$ GeV band for $m_{3/2}$: 50–280 TeV, consistent with its natural allowed range (thanks to the presence of bulk A_0 terms).

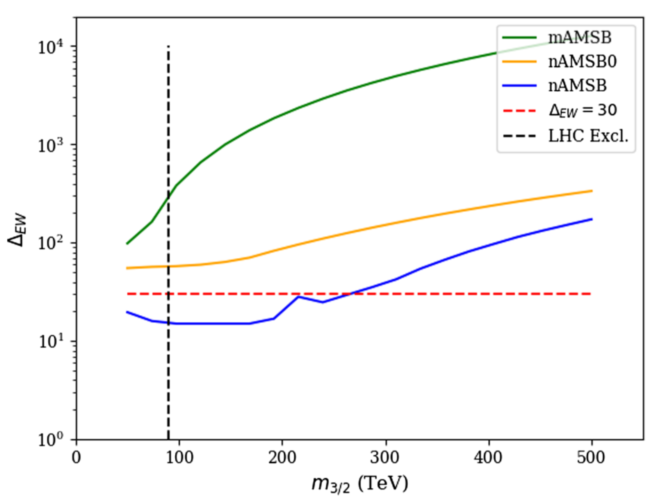

FIG. 5. Plot of $\Delta_{\rm EW}$ vs $m_{3/2}$ along the AMSB model lines. The region below the dashed line $\Delta_{\rm EW} < 30$ is regarded as natural.

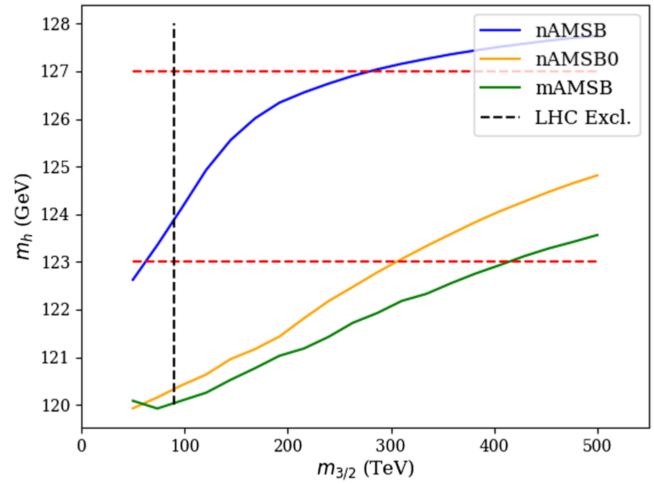

FIG. 6. Plot of m_h vs $m_{3/2}$ along the AMSB model lines. The light Higgs mass is constrained by LHC measurements to lie between the dashed lines, given some theory error on the calculation of m_h.

In Fig. 7, we show various sparticle masses for the nAMSB model line vs $m_{3/2}$. The dark and light blue and lavender lines show the various Higgsino-like EWinos which are typically of order m(Higgsinos) $\sim \mu \sim 250$ GeV. Next heaviest are the winolike EWinos $\tilde{\chi}^0_3$ and $\tilde{\chi}^\pm_2$ shown as green and orange curves. These masses vary from m(winos): 300 to 2000 GeV over the range of $m_{3/2}$ shown, and are, as we shall see, subject to present and future LHC EWino searches.

The black curve shows the gluino mass $m_{\tilde{g}}$: 1.2–10 TeV. We also show the LHC lower bound $m_{\tilde{g}} \sim 2.3$ TeV from gluino pair searches within the context of simplified models by the black-dashed line. The LHC simplified-model results should apply well in the case of nAMSB models

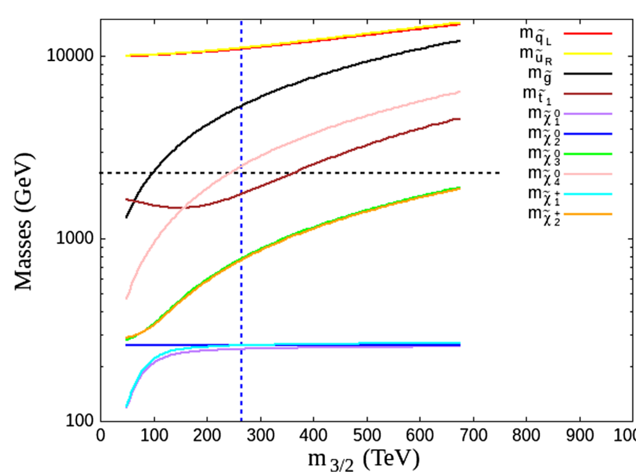

FIG. 7. Plot of sparticle masses vs $m_{3/2}$ along the nAMSB model lines.

since the $\tilde{g}-\tilde{\chi}_1^0$ mass gap is always substantial. The LHC $pp \to \tilde{g}\tilde{g}X$ search limits thus provide a lower bound on allowed nAMSB parameter space with $m_{3/2} \gtrsim 90$ TeV. The blue-dashed line denotes the upper limit on $m_{3/2}$ obtained from naturalness constraints. The lighter top squark mass $m_{\tilde{t}_1}$ is also shown and is beyond the LHC simplified-model limit $m_{\tilde{t}_1} \gtrsim 1.1$ TeV for all $m_{3/2}$ values. First-/second-generation sfermion masses lie around the $m_0(1,2)$ value, so in this case, they would be inaccessible to present and future LHC searches. By combining lower limits from LHC gluino pair searches with upper bounds from naturalness, we expect the allowed $m_{3/2}$ values for nAMSB to lie between $m_{3/2}$:90 and 265 TeV.

IV. LHC PRODUCTION CROSS SECTIONS

In this section, we pivot to prospects for LHC searches for SUSY within the context of the nAMSB model. First, we adopt the computer code PROSPINO [102] to compute the next-to-leading-order production cross sections for various $pp \to SUSY$ reactions, given input from the ISAJET SUSY Les Houches Accord file [103]. Our first results are shown in Fig. 8 where we show cross sections for $pp \to \tilde{g}\tilde{g}$, $\tilde{t}_1\tilde{t}_1^*$ and (summed) EWino pair production vs $m_{3/2}$ along the nAMSB model line. At the top of the plot, we see EWino pair production is dominant and relatively flat vs $m_{3/2}$ since it is dominated by Higgsino pair production and μ is fixed at 250 GeV. The EWino cross section is divided up into summed $\tilde{\chi}_i^0\tilde{\chi}_j^0$, $\tilde{\chi}_i^0\tilde{\chi}_k^\pm$, and $\tilde{\chi}_k^\pm\tilde{\chi}_l^\mp$ production, where $i,j=$ 1–4 and $k,l=$ 1–2. The summed EWino pair cross sections are all comparable and of order $\sim 10^2$ fb. The $pp \to \tilde{t}_1\tilde{t}_1^*$ cross section is also relatively flat, this time reflecting that $m_{\tilde{t}_1}$ hardly changes with increasing $m_{3/2}$ (from Fig. 7). The $pp \to \tilde{g}\tilde{g}$ cross section is falling rapidly with increasing $m_{3/2}$, reflecting that the gluino mass is directly proportional

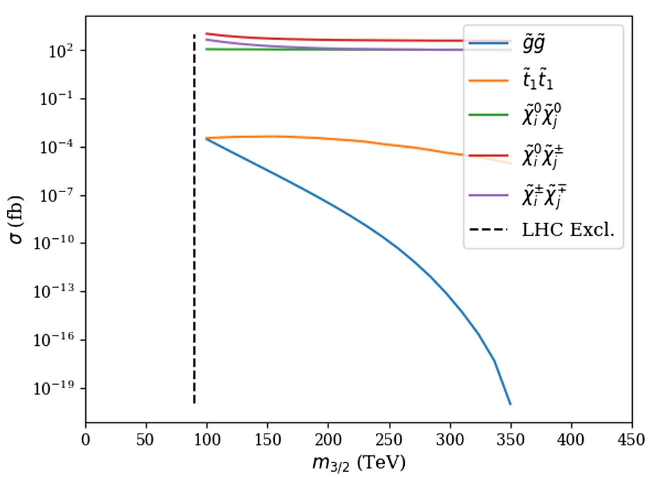

FIG. 8. Plot of $\sigma(pp \to \tilde{g}\tilde{g}, \tilde{t}_1\tilde{t}_1^*)$ and EWino pair production vs $m_{3/2}$ along the nAMSB model line.

to $m_{3/2}$. From the plot, we thus expect most of the reach of the LHC for the nAMSB model will come from EWino pair production rather than from gluino or stop pair production.

There are many subreactions that contribute to the summed EWino pair production cross sections. Each subreaction leads to different final states and thus different SUSY search strategies. In Fig. 9(a), we show the several chargino-chargino pair production reactions vs $m_{3/2}$. The upper blue curve denotes $\tilde{\chi}_1^+\tilde{\chi}_1^-$ where the light charginos are mainly Higgsino-like (except for some substantial mixing at low $m_{3/2}$ where the wino soft term $M_2 \sim \mu$). Given the small $m_{\tilde{\chi}_1^+} - m_{\tilde{\chi}_1^0}$ mass gap, where much of the reaction energy goes into the invisible LSP mass and energy, this reaction is likely to be largely invisible at the LHC. The orange curve denotes charged wino-pair production: $\tilde{\chi}_2^+\tilde{\chi}_2^-$. Given its modest size and the branching fractions from Sec. V, it can be very promising for LHC searches. The third reaction, mixed Higgsino-wino $\tilde{\chi}_1^\pm\tilde{\chi}_2^\mp$ production, occurs at much lower rates.

In Fig. 9(b), we show the ten neutralino pair production reactions $\sigma(pp \to \tilde{\chi}_i^0\tilde{\chi}_j^0)$. By far, the dominant neutralino pair production reaction is $pp \to \tilde{\chi}_1^0\tilde{\chi}_2^0$. This reaction takes place dominantly via s-channel Z^* exchange involving the coupling W_{ij} of Eq. (8.101) of Ref. [104]. The signs of the neutralino mixing elements add constructively in this case leading to a large Higgsino pair production reaction that leads to promising LHC signature in the soft opposite-sign dilepton plus jets plus $\not{E}_T$ channel [105,106] (OSDLJMET). This cross section is flat with increasing $m_{3/2}$ since μ is not a soft term and not expected to directly scan in the landscape, but instead is fixed by whatever solution to the SUSY μ problem attains [107]. The next largest neutralino pair production cross section is $pp \to \tilde{\chi}_2^0\tilde{\chi}_3^0$: wino-Higgsino production, which again has a constructive sign interference along with large mixing terms. Other neutralino pair production reactions are subdominant and typically decreasing with increasing $m_{3/2}$.

In Fig. 9(c), we show $\tilde{\chi}_{1,2}^0\tilde{\chi}_k^\pm$ pair production reactions. The largest $\tilde{\chi}_1^0\tilde{\chi}_1^+$ may again be largely invisible to LHC searches, while the second largest $\tilde{\chi}_2^0\tilde{\chi}_1^+$ can contribute to the OSDLJMET signature mentioned above. The corresponding reactions with negative charginos are comparable to these reactions but somewhat suppressed since they occur mainly via s-channel W^* production, and the LHC is a pp collider which favors positively charged W bosons. The remaining Higgsino-wino production reactions fall with increasing $m_{3/2}$ and are subdominant.

In Fig. 9(d), we show the $\tilde{\chi}_{3,4}^0\tilde{\chi}_k^\pm$ production rates. In this case, wino-pair production $\tilde{\chi}_3^0\tilde{\chi}_2^+$ is dominant but falling as $m_{3/2}$—and hence, M_2—increases in value. The conjugate reaction $\tilde{\chi}_3^0\tilde{\chi}_2^-$ is next largest, followed by $\tilde{\chi}_3^0\tilde{\chi}_1^\pm$. The reactions involving bino production $\tilde{\chi}_4^0$ are all subdominant and may not be so relevant for LHC SUSY searches.

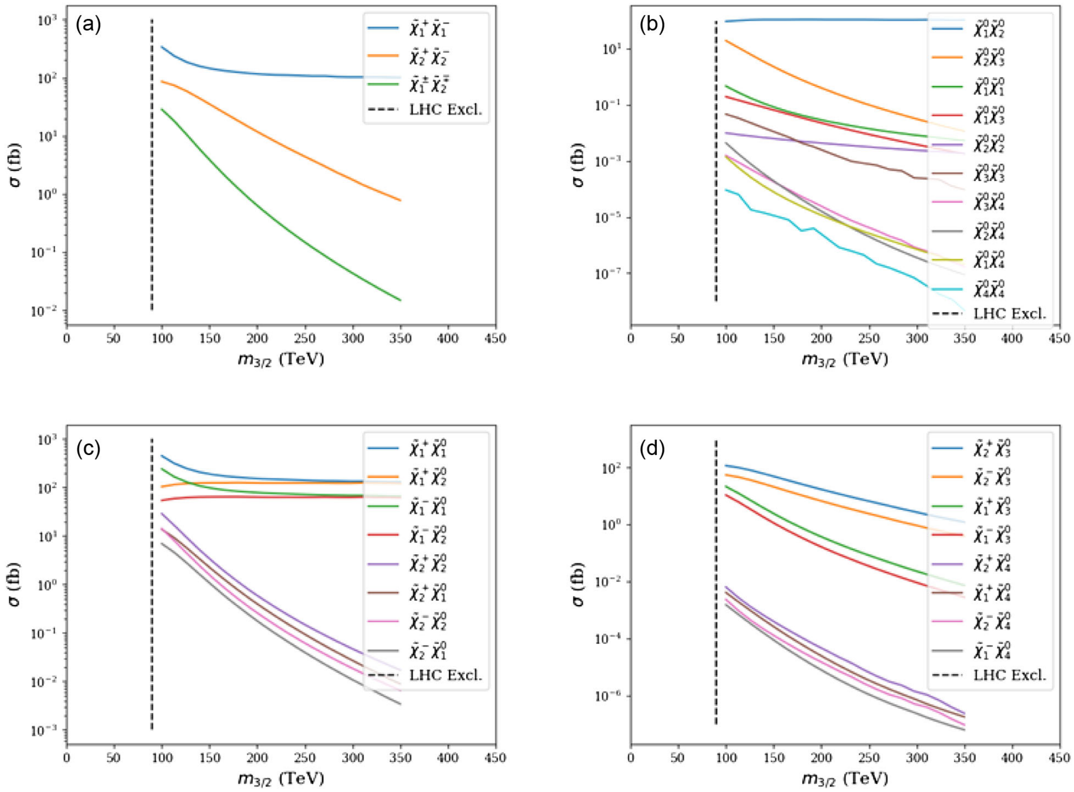

FIG. 9. Plot of various EWino pair production cross sections vs $m_{3/2}$ along the nAMSB model line: (a) chargino pair production, (b) neutralino pair production, (c) chargino-$\tilde{\chi}^0_{12}$ pair production, and (d) chargino-$\tilde{\chi}^0_{3,4}$ pair production.

V. SPARTICLE DECAY MODES

In this section, we wish to comment on some relevant sparticle branching fractions leading to favorable final state search signatures for the LHC. It is evident from the preceding section that EWino pair production is the dominant sparticle production mechanism at the LHC14. The reaction $pp \to \tilde{\chi}^0_1\tilde{\chi}^0_2$ (neutral Higgsino pair production) is dominant, where $\tilde{\chi}^0_2 \to f\bar{f}\tilde{\chi}^0_1$ and where the f's are SM fermions. For the case of nAMSB, the mass gap $m_{\tilde{\chi}^0_2} - m_{\tilde{\chi}^0_1}$ can range up to 50–60 GeV when winos are light, leading to substantial wino-Higgsino mixing for lower values of $m_{3/2} \sim 100$ TeV. The lucrative leptonic branching fraction $\tilde{\chi}^0_2 \to \ell^+\ell^-\tilde{\chi}^0_1$ occurs typically at the 2% level due to competition with other decay modes such as $\tilde{\chi}^0_2 \to \tilde{\chi}^\pm_1 f\bar{f}'$.

The other lucrative production mode from the previous section is wino-pair production $pp \to \tilde{\chi}^0_3\tilde{\chi}^\pm_2$. To assess the expected final states from this reaction, we plot in Fig. 10 the major wino decay branching fractions along the nAMSB model line. In Fig. 10(a), we plot the $BF(\tilde{\chi}^+_2)$ values vs $m_{3/2}$, while in Fig. 10(b), we plot the $BF(\tilde{\chi}^0_3)$ values. From Fig. 10(a), the region with $m_{3/2} \lesssim 90$ TeV is already excluded by LHC $\tilde{g}\tilde{g}$ searches (albeit in the context of simplified models). Below 90 TeV, there is actually a level crossing: Since μ is fixed at 250 GeV, a low enough value of $m_{3/2}$ leads to $m(\text{wino}) < m(\text{Higgsinos})$ and an increased $m_{\tilde{\chi}^+_2} - m_{\tilde{\chi}^+_1}$ mass gap (see Fig. 7) so that $\tilde{\chi}^+_2 \to \tilde{\chi}^+_1 h$ is allowed. Then, as $m_{3/2}$ increases, the mass gap drops (due to wino-Higgsino degeneracy), and the $\tilde{\chi}^+_2 \to \tilde{\chi}^+_1 h$ mode becomes kinematically closed. As $m_{3/2}$ increases beyond $\sim$100 TeV, $\tilde{\chi}^+_2$ becomes winolike, and the mass gap enlarges so that the decay $\tilde{\chi}^+_2 \to \tilde{\chi}^+_1 h$ becomes allowed again. As $m_{3/2}$ increases further, all four decay modes $\tilde{\chi}^+_2 \to \tilde{\chi}^0_1 W^+, \tilde{\chi}^0_2 W^+, \tilde{\chi}^+_1 Z$, and $\tilde{\chi}^+_1 h$ asymptote to $\sim$25%. Thus, we expect the charged wino to decay to Higgsino plus W, Z, or h in a ratio $\sim 2:1:1$. Since the Higgsinos may be quasivisible (depending on decay mode and mass gap), we get wino decay to W, Z, or h + quasivisible Higgsinos as a final state.

In Fig. 10(b), we show the neutral wino $\tilde{\chi}^0_3$ branching fractions along the nAMSB model line. At low $m_{3/2} \sim 90$ TeV near the LHC-excluded region, the neutral winos decay nearly 100% into $\tilde{\chi}^\mp_1 W^\pm$. As $m_{3/2}$ increases, the wino-Higgsino mass gap increases, and decays to $\tilde{\chi}^0_2 Z$ and $\tilde{\chi}^0_1 h$ are allowed and can occur at the $\sim$20% level, while decays to $\tilde{\chi}^\mp_1 W^\pm$ asymptote to $\sim$50%. The remaining branching fraction goes to mixing-suppressed modes. Thus, for wino-pair production, we expect a final state of $VV + MET$, $Vh + MET$, and $hh + MET$ where MET

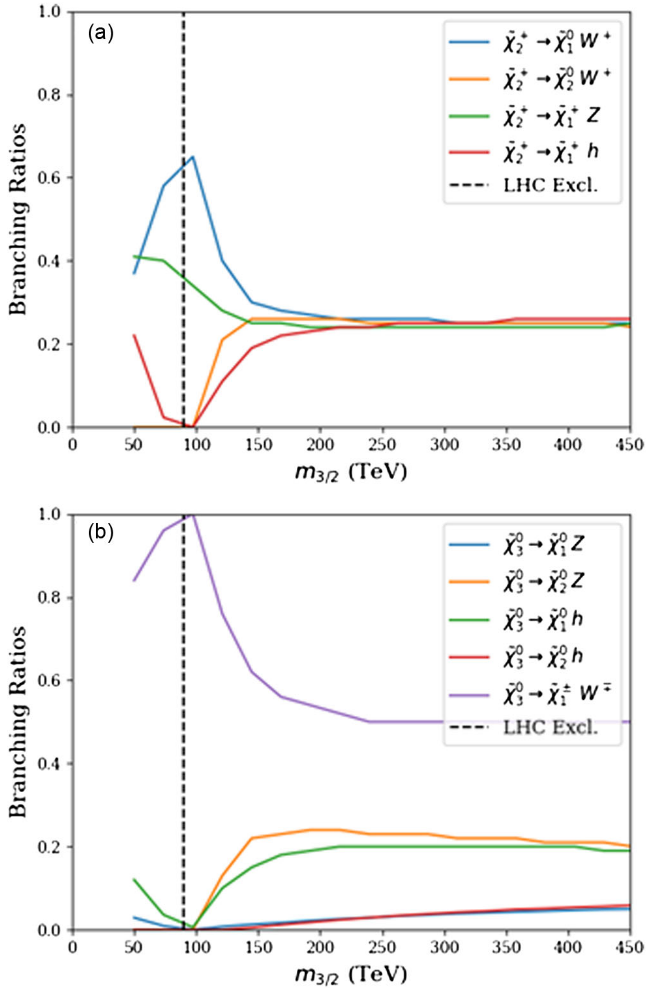

FIG. 10. Plot of charged and neutral wino branching fractions (a) $\mathrm{BF}(\tilde{\chi}_2^+)$ and (b) $\mathrm{BF}(\tilde{\chi}_3^0)$ versus $m_{3/2}$ along the nAMSB model line.

stands for missing transverse energy, and V stands for the vector bosons W and Z. The MET may not really be entirely missing since it may include three-body decay products of the heavier Higgsinos.

In Fig. 11, we plot the light top squark branching fractions $BF(\tilde{t}_1)$ vs $m_{3/2}$ along the nAMSB model line. For very low $m_{3/2}$, $\tilde{t}_1 \to b\tilde{\chi}_2^+$ is dominant where the $\tilde{\chi}_2^\pm$ is a mixed wino-Higgsino. But as $m_{3/2}$ increases, $BF(\tilde{t}_1 \to b\tilde{\chi}_1^+)$ becomes dominant and approaches 50%, not unlike natural SUSY models with gaugino mass unification [108]. The $\tilde{t}_1$ in nAMSB (as in NUHM2 models) is dominantly $\sim\tilde{t}_R$ despite large stop mixing soft term A_t. Also, at larger $m_{3/2}$ values, $BF(\tilde{t}_1 \to t\tilde{\chi}_{1,2}^0)$ each approach $\sim$25%.

VI. LHC-EXCLUDED REGIONS

Certain regions of nAMSB model parameter space seem already excluded by existing LHC13 search limits from Run 2 with $\sim$139 fb^{-1} of integrated luminosity.

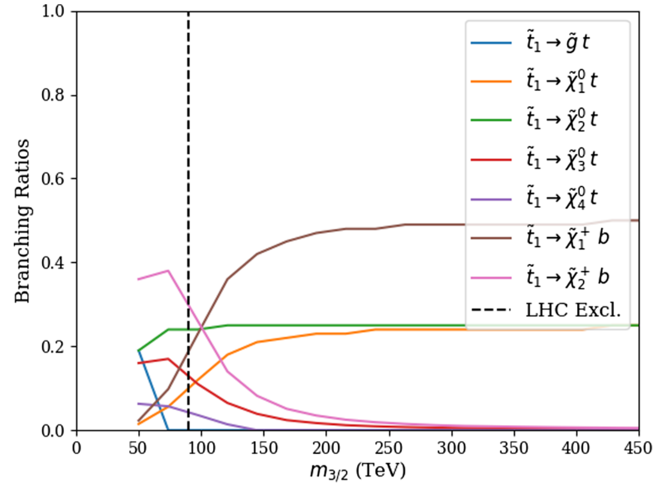

FIG. 11. Plot of top squark branching fractions $\mathrm{BF}(\tilde{t}_1)$ versus $m_{3/2}$ along the nAMSB model line.

A. LHC constraint from gluino pair searches

In the case of gluino pair production, for the bulk of LHC-allowed nAMSB parameter space, we expect $\tilde{g} \to t\tilde{t}_1^*$ followed by further $\tilde{t}_1$ cascade decays. The approximate ATLAS and CMS simplified-model limits for $\tilde{g}\tilde{g}$ production followed by decay to third-generation particles should roughly apply [109–111], and these imply

$$m_{\tilde{g}} \gtrsim 2.3\ \mathrm{TeV}. \tag{11}$$

From Fig. 7, this implies that $m_{3/2} \gtrsim 90$ TeV.

B. LHC constraint from EWino pair production followed by decay to boosted dijets

A recent ATLAS study [112] reports searching for EWino pair production followed by two-body decays to W, Z, or h. These heavy SM objects are assumed to decay hadronically to boosted dijet/fat-jet states which are then identified. A similar study by CMS was also made [113] but with smaller parameter-space exclusion regions. The simplified-model limits presented in Fig. 14(c) of Ref. [112] should roughly apply to our case for wino-pair production $pp \to \tilde{\chi}_2^\pm\tilde{\chi}_3^0$ as shown in Fig. 9(d) followed by decays to vector bosons and Higgs bosons as shown in Fig. 10. The digitized ATLAS exclusion curve is shown in Fig. 12 in the $m(\mathrm{wino})$ vs $m(\mathrm{Higgsinos})$ plane. Our nAMSB model line with $\mu = 250$ GeV is denoted by the horizontal dashed line. From the plot, we would expect that the range $m(\mathrm{wino})$: 625–1000 GeV would be ruled out, corresponding to a range of $m_{3/2}$: 200–350 TeV. For model lines with larger or smaller values of μ, the exclusion region changes accordingly in Fig. 12.

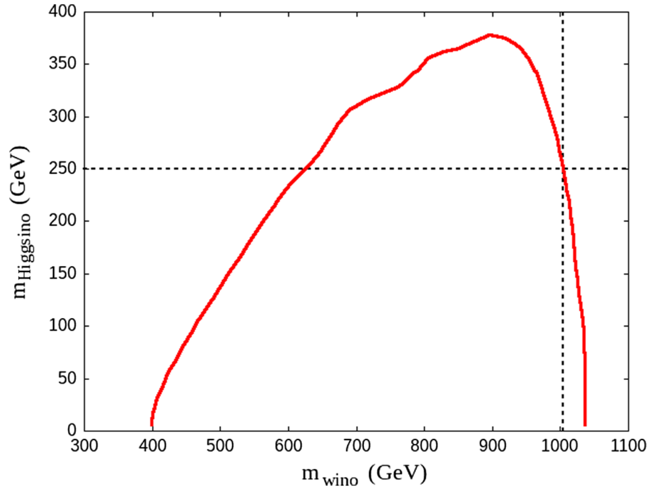

FIG. 12. Allowed/excluded regions of the m(wino) vs m(Higgsinos) plane from ATLAS analysis of EWino pair production followed by decay to W, Z, h with decay to boosted dijets.

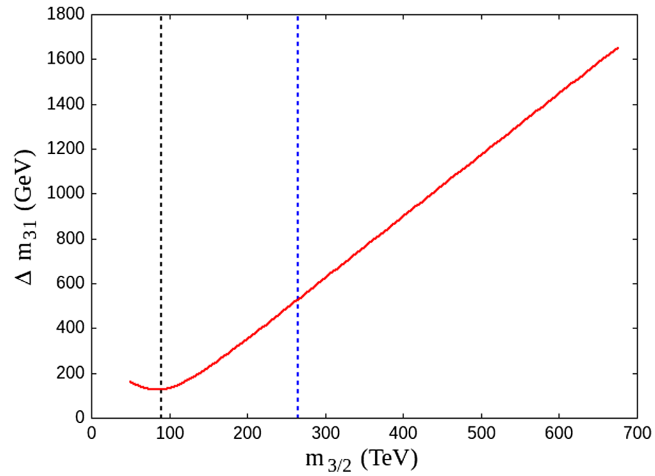

FIG. 13. Variation of $\Delta m_{31} = m_{\tilde{\chi}^0_3} - m_{\tilde{\chi}^0_1}$ vs $m_{3/2}$. The region left of the black-dashed curve is excluded by LHC13 gluino pair searches, and the region to the right of the blue-dashed line is unnatural with $\Delta_{\rm EW} \gtrsim 30$.

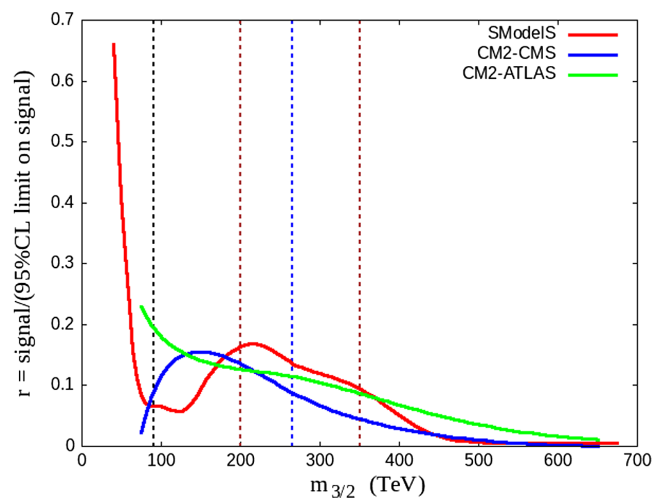

FIG. 14. Plot of r from SModelS and CheckMATE2 vs $m_{3/2}$ along the nAMSB model line.

C. LHC constraints from SModelS/CheckMATE2 analysis

To test for further limits on nAMSB parameter space, we employ two recent recasting softwares: SModelS [114–116] and CheckMATE2 [117,118] to study the impact of the current searches on nAMSB parameter space. SModelS is a popular tool for interpreting simplified-model results from the LHC. It decomposes beyond the Standard Model (BSM) collider signatures presenting a Z_2-like symmetry into simplified model spectrum (SMS) topologies and compares the BSM predictions for the LHC in a model-independent framework with the relevant experimental constraints. The main variable for comparison of a BSM theory to the LHC experimental searches is the r ratio, which is defined as the ratio of the expected $\sigma \times BR$ for a specific final state to the corresponding upper limit on the $\sigma \times BR \times \epsilon$ (where ϵ is the acceptance efficiency provided by the experimental paper). CheckMATE2 is reinterpretation software for interpreting LHC results for all BSM models. It is based on recasting the full experimental analyses using events after full Monte Carlo simulation, hadronization, and detector smearing of the final state objects and implementing the cuts as in the experimental analyses. It provides the r value defined as the ratio of the expected number of events from the signal, after implementing all cuts, to the 95% CL upper limit from the experimental result. In both cases, for a BSM model to be allowed by current constraints, one requires $r < 1$.

The wino-Higgsino mass gap quantified by $\Delta m_{31} = m_{\tilde{\chi}^0_3} - m_{\tilde{\chi}^0_1}$ increases with $m_{3/2}$ as seen in Fig. 13. Figure 14 shows the variation of the highest r value obtained from SModelS and CheckMATE2 for the $\sqrt{s} = 13$ TeV results from the LHC. The highest r value defined as the ratio of the signal over the 95% CL upper limit from the signal region is plotted against $m_{3/2}$. The red dotted lines denote the constraints from the ATLAS search of boosted hadronically decaying bosons + $\not\!\!E_T$ [112], while the black dotted line denotes the bound from the gluino searches implying $m_{3/2} \geq$ 90 TeV as discussed in Secs. VI B and VI A, respectively.

For the constraints from the CheckMATE2 CMS results (blue), we observe the tightest constraints arise from the multilepton $(2/3) + \not\!\!E_T$ searches [119] for $m_{3/2} \sim$ 150 TeV with r value ~0.15, and it falls off on either side of the peak. This is due to other searches gaining more importance such as searches for $\geq 4\ell + \not\!\!E_T$ for larger mass gaps between the winolike and Higgsino-like neutralino. From the CheckMATE2 ATLAS result (green), the r value decreases with increasing $m_{3/2}$ from $r = 0.25$ arising from the hadronic searches of squarks and gluinos [120].

From SModelS (red), the most stringent constraint occurs at $m_{3/2} < 100$ TeV from searches of three leptons + $\not{E}_T$ [121]. For the $m_{3/2} = 100$–250 TeV range, the most stringent constraints arise from the boosted hadronically decaying diboson + $\not{E}_T$ searches; the multilepton searches involving two or three leptons + $\not{E}_T$ [121,122] are the most sensitive searches near the peak at $m_{3/2} \sim 225$ TeV. For higher $m_{3/2} = 250$–400 TeV, the dominant constraints arise from the multilepton searches, and subdominant constraints arise from the boosted hadronically decaying dibosons + $\not{E}_T$. As $m_{3/2}$ increases, the multijet + $\not{E}_T$ [123] searches start constraining the parameter space dominantly. However, the r value always remains less than 1; thus, the remaining allowed range of $m_{3/2} \sim 90$–200 TeV appears to be presently allowed.

D. LHC-allowed nAMSB parameter space

Our final allowed nAMSB model line parameter space is shown in Fig. 15. The left gray shaded region is excluded by LHC gluino search limits, while the central gray shaded region is excluded by the ATLAS limits on EWino pair production followed by decay to two boosted dijet final states. The naturalness limit is denoted by the vertical dashed line within the central excluded band: The region to the right is unnatural, and thus highly unlikely (but not impossible) to emerge from the landscape. The unshaded region extends from $m_{3/2}$: 90 to 200 TeV and is thus the presently allowed parameter space. For convenience, we display again the sparticle masses along our nAMSB model line. The remaining SUSY particle spectrum for $m_{3/2} \sim 90$–200 TeV should provide a target for future LHC searches seeking to discover or to rule out natural AMSB.

VII. PROSPECTS FOR nAMSB AT RUN 3 AND HI-LUMI LHC SEARCHES

A. LHC Higgsino pair production search

1. Soft opposite-sign dilepton, jet + *MET* search

In models with light Higgsinos, as in natural SUSY, a compelling LHC search reaction [124] is $pp \to \tilde{\chi}_1^0\tilde{\chi}_2^0$ followed by $\tilde{\chi}_2^0 \to \ell^+\ell^-\tilde{\chi}_1^0$, where the dilepton pair is energetically rather soft since its invariant mass a kinematically bounded by $m_{\tilde{\chi}_2^0} - m_{\tilde{\chi}_1^0}$. By triggering on hard initial state QCD radiation [105,106], such soft dilepton + $\not{E}_T$ events can be searched for at the LHC. Prospects for soft dileptons, jets + $\not{E}_T$ events (soft OSDLJMET), at the LHC have been presented in the Higgsino discovery plane [125] and in Ref. [126] where new angular cuts were proposed to aid in discovery. Recent search results from CMS [122] and ATLAS [127] have been presented.

The soft OSDJMET signal is a particularly compelling signal for SUSY in the nAMSB model in light of the large $pp \to \tilde{\chi}_1^0\tilde{\chi}_2^0$ cross section from Fig. 9(b). A distinguishing feature of the nAMSB model compared to models with gaugino mass unification or mirage mediation is the relatively larger $\Delta m_{21} \equiv m_{\tilde{\chi}_2^0} - m_{\tilde{\chi}_1^0}$ mass gap ranging from ~15 to 60 GeV for nAMSB as shown in Fig. 16 (due to the larger wino-Higgsino mixing from light winos). Current searches from CMS and ATLAS probe a maximal μ value of ~200 GeV for mass gaps $\Delta m_{21} \sim 10$ GeV. Future ATLAS and CMS probes at the HL LHC with 3000 fb^{-1} can probe to $\mu \sim 300$ GeV [128], and the improved angular cuts may allow the HL LHC to probe as high as $\mu \sim 325$ GeV [126]. It should be noted that both ATLAS and CMS seem to have a 2σ excess in this channel at present with 139 fb^{-1} of integrated luminosity. In nAMSB with a

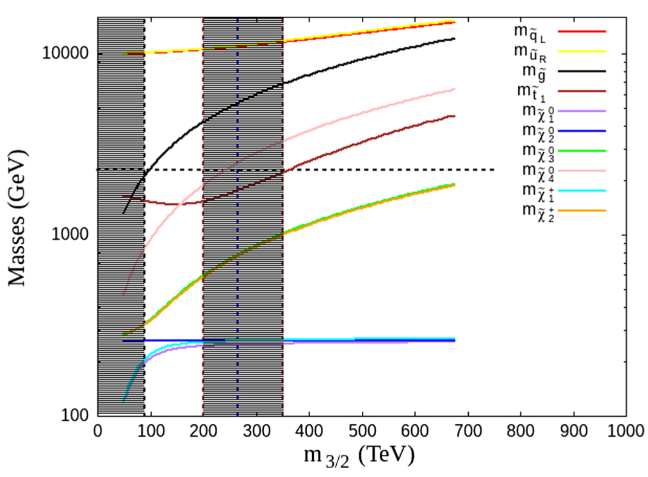

FIG. 15. Allowed/excluded regions of our nAMSB model line along with various sparticle masses.

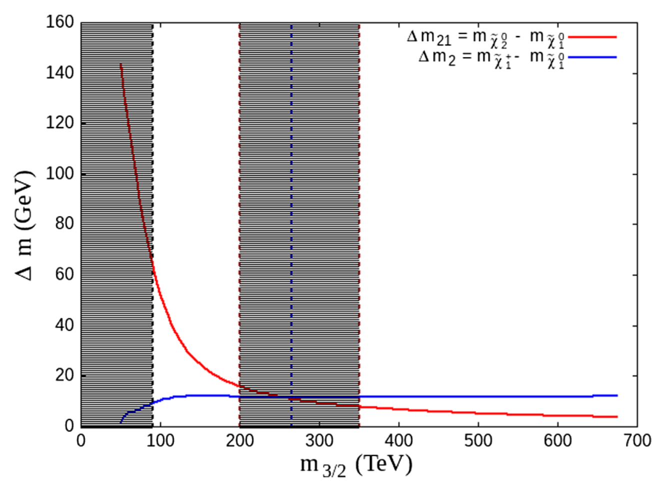

FIG. 16. Plot of $m_{\tilde{\chi}_2^0} - m_{\tilde{\chi}_1^0}$ and $m_{\tilde{\chi}_1^+} - m_{\tilde{\chi}_1^0}$ mass gaps vs $m_{3/2}$ along the nAMSB model line.

larger $m_{\tilde{\chi}_1^+} - m_{\tilde{\chi}_1^0}$ mass gap, soft trilepton plus jet $+ \not{E}_T$ signatures should also be available from $\tilde{\chi}_1^\pm \tilde{\chi}_2^0$ production.

B. LHC wino-pair production search

1. Boosted hadronic signature

The rather light winos expected from the allowed parameter-space window in Fig. 15 provide an inviting target for LHC wino-pair production searches. In the case of $pp \to \tilde{\chi}_2^\pm \tilde{\chi}_3^0$ production, the relevant signatures occur in the $VV + \not{E}_T$, $Vh + \not{E}_T$, and $hh + \not{E}_T$ channels, where $V = W$ or Z. While the strong ATLAS limits from boosted V or $H \to jj$ already exclude $m_{3/2}$: 200–350 TeV, a search for nonboosted multijets $+ \not{E}_T$ may be warranted for electroweak-produced wino pairs. These searches may be augmented by searching for the presence of $h \to b\bar{b}$ and $V \to$ leptons in the signal events. New targeted analyses using Run 2 data or forthcoming Run 3 data may even be able to close this allowed window (or else discover nAMSB SUSY). Certainly, the allowed window in nAMSB parameter space can be closed by analysis of HL-LHC data.

2. Same-sign diboson signature

The other lucrative search channel for wino-pair production followed by decay to light Higgsinos is the same-sign diboson channel (SSdB) [129], where $pp \to \tilde{\chi}_2^\pm \tilde{\chi}_3^0$ will be followed by $\tilde{\chi}_2^\pm \to W^\pm \tilde{\chi}_{1,2}^0$ and $\tilde{\chi}_3^0 \to W^\pm \tilde{\chi}_1^\mp$. These production and decay modes lead equally to $W^+W^- + \not{E}_T$ and $W^\pm W^\pm + \not{E}_T$ final states where the former has large SM backgrounds from WW and $t\bar{t}$ production while SM backgrounds for the latter SSdB signature are far smaller [129–131]. This relatively jet-free (only jets from initial state QCD radiation) signature is distinct from the usual same-sign dilepton signature arising from gluino and squark pair production which should be accompanied by many hard final state jets.

The reach of the HL LHC for the natural SUSY SSdB signature has been computed in Ref. [131] where peak signal cross sections after cuts reach the 0.03 fb level compared to total SM backgrounds of 0.005 fb. Whereas the present reach of the LHC with 139 fb^{-1} is minimal (for the harder, high-luminosity cuts advocated in Ref. [131]), the low wino mass $m(\mathrm{wino}) \sim 300$–600 GeV region should be accessible to the LHC Run 3 and HL-LHC datasets in the 300–3000 fb^{-1} regime. Alternatively, a fresh analysis by the experimental groups using softer cuts for the low wino mass region is clearly warranted. So far, it seems no dedicated analysis of the SSdB signature from natural SUSY has been undertaken.

C. LHC stop pair production search: $pp \to \tilde{t}_1 \tilde{t}_1^*$

Another SUSY search channel for the nAMSB model is via light top squark pair production $pp \to \tilde{t}_1 \tilde{t}_1^*$ followed by $\tilde{t}_1 \to b\tilde{\chi}_1^+$ at ∼50% and $\tilde{t}_1 \to t\tilde{\chi}_{1,2}^0$ each at ∼25%. The reach of the HL LHC for light top squarks with these decay modes has been recently evaluated [100]. The 5σ discovery reach of the HL LHC with 3000 fb^{-1} was found to extend to $m_{\tilde{t}_1} \sim 1.7$ TeV, while the 95% CL reach extended to $m_{\tilde{t}_1} \sim 2$ TeV. These sorts of search limits performed within the NUHM2 model are expected to pertain also to stop pair production within the nAMSB model.

VIII. SUMMARY AND CONCLUSIONS

Supersymmetric models with anomaly-mediated SUSY breaking are well motivated in several different SUSY breaking scenarios. In charged SUSY breaking (AMSB0), gauginos and A terms have suppressed gravity-mediated masses but can gain dominant AMSB masses, while scalar masses assume their usual gravity-mediated form. In the RS AMSB model with sequestered SUSY breaking, gaugino masses, A terms, and scalar masses all have the AMSB form, leading to negative squared slepton masses. Further bulk scalar mass contributions are required for a viable model. The phenomenology of mAMSB models is characterized by a wino LSP and winolike WIMP dark matter. The minimal phenomenological version of these models seems to be triply ruled out by (1) the difficulty to generate $m_h \sim 125$ GeV unless huge, unnatural third-generation bulk scalar masses are included, (2) the presence of winolike WIMP dark matter, which seems excluded by direct and indirect dark matter detection limits, and (3) the large, unnatural value of μ—and hence, large Δ_{EW}—that such models possess, even for weak-scale soft terms. Rather minor tweaks to the mAMSB model, already suggested in the original work of RS [23], ameliorate these problems: nonuniversal bulk scalar Higgs masses and bulk A terms. While AMSB0 with nonuniversal scalar masses still seems ruled out (due to $A_0 \sim 0$ and hence, too low m_h values), the natural AMSB model is both natural and can accommodate $m_h \sim 125$ GeV. In nAMSB, while the wino is still the lightest gaugino, the Higgsinos are instead the lightest EWinos. The dark matter issues can be resolved by postulating mixed axion-Higgsino-like WIMP dark matter which is mainly composed of axions [68].

In this work, we investigated in some detail the LHC constraints on natural AMSB models. LHC gluino mass limits already require a gravitino mass $m_{3/2} \gtrsim 90$ TeV. The presence of relatively light winos with mass $m(\mathrm{wino}) \sim 300$–800 GeV implies the model is susceptible to ATLAS/CMS searches for two boosted dijets $+ \not{E}_T$. Recent ATLAS results seem to rule out $m_{3/2} \sim 200$–350 TeV, whereas naturalness ($\Delta_{\mathrm{EW}} \lesssim 30$) requires $m_{3/2} \lesssim 265$ TeV. The combined constraints leave an open lower mass window of $m_{3/2} \sim 90$–200 TeV. This lower mass window may soon be excluded (or else nAMSB may be discovered) by a combination of (1) soft OS dilepton plus jet $+ \not{E}_T$ (OSDLJMET) searches which arise from Higgsino pair production, (2) nonboosted hadronically decaying wino-pair production searches, and (3) jet-free same-sign diboson searches which are a characteristic signature of wino-pair production followed by wino decay to $W+$ Higgsinos. Some excess above SM background in the OSDLJMET channel already seems to be present in both ATLAS and CMS data [122,127].

ACKNOWLEDGMENTS

This material is based upon work supported by the U.S. Department of Energy, Office of Science, Office of High Energy Physics under Award No. DE-SC-0009956. V. B. gratefully acknowledges support from the William F. Vilas estate.

[1] D. J. H. Chung, L. L. Everett, G. L. Kane, S. F. King, J. D. Lykken, and L.-T. Wang, The soft supersymmetry breaking Lagrangian: Theory and applications, Phys. Rep. **407**, 1 (2005).
[2] G. F. Giudice, M. A. Luty, H. Murayama, and R. Rattazzi, Gaugino mass without singlets, J. High Energy Phys. 12 (1998) 027.
[3] E. Witten, Dynamical breaking of supersymmetry, Nucl. Phys. **B188**, 513 (1981).
[4] M. Dine and J. D. Mason, Supersymmetry and its dynamical breaking, Rep. Prog. Phys. **74**, 056201 (2011).
[5] I. Affleck, M. Dine, and N. Seiberg, Dynamical supersymmetry breaking in four-dimensions and its phenomenological implications, Nucl. Phys. **B256**, 557 (1985).
[6] A. E. Nelson, A viable model of dynamical supersymmetry breaking in the hidden sector, Phys. Lett. B **369**, 277 (1996).
[7] G. Lopes Cardoso and B. A. Ovrut, Supersymmetric calculation of mixed Kahler gauge and mixed Kahler-Lorentz anomalies, Nucl. Phys. **B418**, 535 (1994).
[8] J. A. Bagger, T. Moroi, and E. Poppitz, Anomaly mediation in supergravity theories, J. High Energy Phys. 04 (2000) 009.
[9] L. J. Dixon, V. Kaplunovsky, and J. Louis, Moduli dependence of string loop corrections to gauge coupling constants, Nucl. Phys. **B355**, 649 (1991).
[10] M. Dine and D. MacIntire, Supersymmetry, naturalness, and dynamical supersymmetry breaking, Phys. Rev. D **46**, 2594 (1992).
[11] V. S. Kaplunovsky and J. Louis, Model independent analysis of soft terms in effective supergravity and in string theory, Phys. Lett. B **306**, 269 (1993).
[12] V. Kaplunovsky and J. Louis, Field dependent gauge couplings in locally supersymmetric effective quantum field theories, Nucl. Phys. **B422**, 57 (1994).
[13] J. D. Wells, Implications of supersymmetry breaking with a little hierarchy between gauginos and scalars, in *Proceedings of the 11th International Conference on Supersymmetry and the Unification of Fundamental Interactions, Tucson, Arizona, 2003* (2003), arXiv:hep-ph/0306127.
[14] J. D. Wells, PeV-scale supersymmetry, Phys. Rev. D **71**, 015013 (2005).
[15] N. Arkani-Hamed and S. Dimopoulos, Supersymmetric unification without low energy supersymmetry and signatures for fine-tuning at the LHC, J. High Energy Phys. 06 (2005) 073.
[16] N. Arkani-Hamed, S. Dimopoulos, G. F. Giudice, and A. Romanino, Aspects of split supersymmetry, Nucl. Phys. **B709**, 3 (2005).
[17] A. Arvanitaki, N. Craig, S. Dimopoulos, and G. Villadoro, Mini-split, J. High Energy Phys. 02 (2013) 126.
[18] G. F. Giudice and A. Strumia, Probing high-scale and split supersymmetry with Higgs mass measurements, Nucl. Phys. **B858**, 63 (2012).
[19] M. Carena and H. E. Haber, Higgs boson theory and phenomenology, Prog. Part. Nucl. Phys. **50**, 63 (2003).
[20] H. Baer, V. Barger, and A. Mustafayev, Implications of a 125 GeV Higgs scalar for LHC SUSY and neutralino dark matter searches, Phys. Rev. D **85**, 075010 (2012).
[21] M. Dine, R. G. Leigh, and A. Kagan, Flavor symmetries and the problem of squark degeneracy, Phys. Rev. D **48**, 4269 (1993).
[22] J. L. Feng, T. Moroi, L. Randall, M. Strassler, and S.-f. Su, Discovering supersymmetry at the Tevatron in wino LSP scenarios, Phys. Rev. Lett. **83**, 1731 (1999).
[23] L. Randall and R. Sundrum, Out of this world supersymmetry breaking, Nucl. Phys. **B557**, 79 (1999).
[24] M. Kawasaki, K. Kohri, T. Moroi, and A. Yotsuyanagi, Big-bang nucleosynthesis and gravitino, Phys. Rev. D **78**, 065011 (2008).
[25] J. Pradler and F. D. Steffen, Thermal gravitino production and collider tests of leptogenesis, Phys. Rev. D **75**, 023509 (2007).
[26] T. Moroi and L. Randall, Wino cold dark matter from anomaly mediated SUSY breaking, Nucl. Phys. **B570**, 455 (2000).
[27] K. J. Bae, H. Baer, V. Barger, and R. W. Deal, The cosmological moduli problem and naturalness, J. High Energy Phys. 02 (2022) 138.
[28] M. K. Gaillard and B. D. Nelson, Quantum induced soft supersymmetry breaking in supergravity, Nucl. Phys. **B588**, 197 (2000).
[29] A. Anisimov, M. Dine, M. Graesser, and S. D. Thomas, Brane world SUSY breaking, Phys. Rev. D **65**, 105011 (2002).
[30] A. Anisimov, M. Dine, M. Graesser, and S. D. Thomas, Brane world SUSY breaking from string/M theory, J. High Energy Phys. 03 (2002) 036.
[31] M. A. Luty, 2004 TASI lectures on supersymmetry breaking, arXiv:hep-th/0509029.
[32] D. R. T. Jones and G. G. Ross, Anomaly mediation and dimensional transmutation, Phys. Lett. B **642**, 540 (2006).

[33] M. Dine and N. Seiberg, Comments on quantum effects in supergravity theories, J. High Energy Phys. 03 (2007) 040.
[34] S. P. de Alwis, On anomaly mediated SUSY breaking, Phys. Rev. D **77**, 105020 (2008).
[35] H. Baer, S. de Alwis, K. Givens, S. Rajagopalan, and H. Summy, Gaugino anomaly mediated SUSY breaking: Phenomenology and prospects for the LHC, J. High Energy Phys. 05 (2010) 069.
[36] D.-W. Jung and J. Y. Lee, Anomaly-mediated supersymmetry breaking demystified, J. High Energy Phys. 03 (2009) 123.
[37] D. Sanford and Y. Shirman, Anomaly mediation from Randall-Sundrum to Dine-Seiberg, Phys. Rev. D **83**, 125020 (2011).
[38] J. P. Conlon, M. Goodsell, and E. Palti, Anomaly mediation in superstring theory, Fortschr. Phys. **59**, 5 (2011).
[39] F. D'Eramo, J. Thaler, and Z. Thomas, The two faces of anomaly mediation, J. High Energy Phys. 06 (2012) 151.
[40] F. D'Eramo, J. Thaler, and Z. Thomas, Anomaly mediation from unbroken supergravity, J. High Energy Phys. 09 (2013) 125.
[41] M. Dine and P. Draper, Anomaly mediation in local effective theories, J. High Energy Phys. 02 (2014) 069.
[42] S. P. de Alwis, AMSB and the logic of spontaneous SUSY breaking, J. High Energy Phys. 01 (2013) 006.
[43] K. Harigaya and M. Ibe, Anomaly mediated gaugino mass and path-integral measure, Phys. Rev. D **90**, 085028 (2014).
[44] M. Luty and R. Sundrum, Anomaly mediated supersymmetry breaking in four-dimensions, naturally, Phys. Rev. D **67**, 045007 (2003).
[45] M. Dine, P. J. Fox, E. Gorbatov, Y. Shadmi, Y. Shirman, and S. D. Thomas, Visible effects of the hidden sector, Phys. Rev. D **70**, 045023 (2004).
[46] M. Ibe, K. I. Izawa, Y. Nakayama, Y. Shinbara, and T. Yanagida, Conformally sequestered SUSY breaking in vector-like gauge theories, Phys. Rev. D **73**, 015004 (2006).
[47] H. Murayama, Y. Nomura, and D. Poland, More visible effects of the hidden sector, Phys. Rev. D **77**, 015005 (2008).
[48] T. Gherghetta, G. F. Giudice, and J. D. Wells, Phenomenological consequences of supersymmetry with anomaly induced masses, Nucl. Phys. **B559**, 27 (1999).
[49] J. L. Feng and T. Moroi, Supernatural supersymmetry: Phenomenological implications of anomaly mediated supersymmetry breaking, Phys. Rev. D **61**, 095004 (2000).
[50] F. E. Paige and J. D. Wells, Anomaly mediated SUSY breaking at the LHC, arXiv:hep-ph/0001249.
[51] H. Baer, J. K. Mizukoshi, and X. Tata, Reach of the CERN LHC for the minimal anomaly mediated SUSY breaking model, Phys. Lett. B **488**, 367 (2000).
[52] A. J. Barr, C. G. Lester, M. A. Parker, B. C. Allanach, and P. Richardson, Discovering anomaly mediated supersymmetry at the LHC, J. High Energy Phys. 03 (2003) 045.
[53] B. C. Allanach, T. J. Khoo, and K. Sakurai, Interpreting a 1 fb^{-1} ATLAS search in the minimal anomaly mediated supersymmetry breaking model, J. High Energy Phys. 11 (2011) 132.
[54] E. Bagnaschi *et al.*, Likelihood analysis of the minimal AMSB model, Eur. Phys. J. C **77**, 268 (2017).
[55] H. Baer, V. Barger, D. Mickelson, and M. Padeffke-Kirkland, SUSY models under siege: LHC constraints and electroweak fine-tuning, Phys. Rev. D **89**, 115019 (2014).
[56] H. Baer, V. Barger, P. Huang, A. Mustafayev, and X. Tata, Radiative natural SUSY with a 125 GeV Higgs boson, Phys. Rev. Lett. **109**, 161802 (2012).
[57] H. Baer, V. Barger, P. Huang, D. Mickelson, A. Mustafayev, and X. Tata, Radiative natural supersymmetry: Reconciling electroweak fine-tuning and the Higgs boson mass, Phys. Rev. D **87**, 115028 (2013).
[58] A. Arbey, M. Battaglia, A. Djouadi, F. Mahmoudi, and J. Quevillon, Implications of a 125 GeV Higgs for supersymmetric models, Phys. Lett. B **708**, 162 (2012).
[59] H. Baer, V. Barger, and A. Mustafayev, Neutralino dark matter in mSUGRA/CMSSM with a 125 GeV light Higgs scalar, J. High Energy Phys. 05 (2012) 091.
[60] T. Cohen, M. Lisanti, A. Pierce, and T. R. Slatyer, Wino dark matter under siege, J. Cosmol. Astropart. Phys. 10 (2013) 061.
[61] J. Fan and M. Reece, In wino veritas? Indirect searches shed light on neutralino dark matter, J. High Energy Phys. 10 (2013) 124.
[62] H. Baer, V. Barger, and H. Serce, SUSY under siege from direct and indirect WIMP detection experiments, Phys. Rev. D **94**, 115019 (2016).
[63] K. J. Bae, H. Baer, A. Lessa, and H. Serce, Mixed axion-wino dark matter, Front. Phys. **3**, 49 (2015).
[64] H. Baer, V. Barger, and D. Sengupta, Anomaly mediated SUSY breaking model retrofitted for naturalness, Phys. Rev. D **98**, 015039 (2018).
[65] P. Slavich *et al.*, Higgs-mass predictions in the MSSM and beyond, Eur. Phys. J. C **81**, 450 (2021).
[66] J. R. Ellis, K. A. Olive, and Y. Santoso, The MSSM parameter space with nonuniversal Higgs masses, Phys. Lett. B **539**, 107 (2002).
[67] H. Baer, A. Mustafayev, S. Profumo, A. Belyaev, and X. Tata, Direct, indirect and collider detection of neutralino dark matter in SUSY models with non-universal Higgs masses, J. High Energy Phys. 07 (2005) 065.
[68] H. Baer, A. Lessa, S. Rajagopalan, and W. Sreethawong, Mixed axion/neutralino cold dark matter in supersymmetric models, J. Cosmol. Astropart. Phys. 06 (2011) 031.
[69] K. J. Bae, H. Baer, and E. J. Chun, Mixed axion/neutralino dark matter in the SUSY DFSZ axion model, J. Cosmol. Astropart. Phys. 12 (2013) 028.
[70] R. Bousso and J. Polchinski, Quantization of four form fluxes and dynamical neutralization of the cosmological constant, J. High Energy Phys. 06 (2000) 006.
[71] L. Susskind, The anthropic landscape of string theory, arXiv:hep-th/0302219.
[72] M. R. Douglas and S. Kachru, Flux compactification, Rev. Mod. Phys. **79**, 733 (2007).
[73] M. R. Douglas, The statistics of string/M theory vacua, J. High Energy Phys. 05 (2003) 046.
[74] S. Ashok and M. R. Douglas, Counting flux vacua, J. High Energy Phys. 01 (2004) 060.

[75] W. Taylor and Y.-N. Wang, The F-theory geometry with most flux vacua, J. High Energy Phys. 12 (2015) 164.
[76] S. Weinberg, Anthropic bound on the cosmological constant, Phys. Rev. Lett. **59**, 2607 (1987).
[77] G. F. Giudice and A. Romanino, Split supersymmetry, Nucl. Phys. **B699**, 65 (2004); **B706**, 487(E) (2005).
[78] E. Bagnaschi, G. F. Giudice, P. Slavich, and A. Strumia, Higgs mass and unnatural supersymmetry, J. High Energy Phys. 09 (2014) 092.
[79] N. Arkani-Hamed, A. Gupta, D. E. Kaplan, N. Weiner, and T. Zorawski, Simply unnatural supersymmetry, arXiv:1212.6971.
[80] H. Baer, V. Barger, D. Martinez, and S. Salam, Radiative natural supersymmetry emergent from the string landscape, J. High Energy Phys. 03 (2022) 186.
[81] V. Agrawal, S. M. Barr, J. F. Donoghue, and D. Seckel, Viable range of the mass scale of the standard model, Phys. Rev. D **57**, 5480 (1998).
[82] H. Baer, V. Barger, D. Martinez, and S. Salam, Fine-tuned vs. natural supersymmetry: What does the string landscape predict?, J. High Energy Phys. 09 (2022) 125.
[83] G. L. Kane, C. F. Kolda, L. Roszkowski, and J. D. Wells, Study of constrained minimal supersymmetry, Phys. Rev. D **49**, 6173 (1994).
[84] L. J. Hall and Y. Nomura, Spread supersymmetry, J. High Energy Phys. 01 (2012) 082.
[85] V. Barger, J. Jiang, P. Langacker, and T. Li, Non-canonical gauge coupling unification in high-scale supersymmetry breaking, Nucl. Phys. **B726**, 149 (2005).
[86] B. S. Acharya, K. Bobkov, G. L. Kane, J. Shao, and P. Kumar, The G_2-MSSM: An M theory motivated model of particle physics, Phys. Rev. D **78**, 065038 (2008).
[87] M. R. Douglas, Statistical analysis of the supersymmetry breaking scale, arXiv:hep-th/0405279.
[88] H. P. Nilles and P. K. S. Vaudrevange, Geography of fields in extra dimensions: String theory lessons for particle physics, Mod. Phys. Lett. A **30**, 1530008 (2015).
[89] H. Baer, V. Barger, S. Salam, and D. Sengupta, String landscape guide to soft SUSY breaking terms, Phys. Rev. D **102**, 075012 (2020).
[90] H. Baer, V. Barger, H. Serce, and K. Sinha, Higgs and superparticle mass predictions from the landscape, J. High Energy Phys. 03 (2018) 002.
[91] K. Choi, A. Falkowski, H. P. Nilles, M. Olechowski, and S. Pokorski, Stability of flux compactifications and the pattern of supersymmetry breaking, J. High Energy Phys. 11 (2004) 076.
[92] K. Choi, A. Falkowski, H. P. Nilles, and M. Olechowski, Soft supersymmetry breaking in KKLT flux compactification, Nucl. Phys. **B718**, 113 (2005).
[93] H. Baer, V. Barger, H. Serce, and X. Tata, Natural generalized mirage mediation, Phys. Rev. D **94**, 115017 (2016).
[94] H. Baer, V. Barger, and D. Sengupta, Mirage mediation from the landscape, Phys. Rev. Res. **2**, 013346 (2020).
[95] H. Baer, V. Barger, X. Tata, and K. Zhang, Prospects for heavy neutral SUSY HIGGS scalars in the hMSSM and natural SUSY at LHC upgrades, Symmetry **14**, 2061 (2022).
[96] H. Baer, V. Barger, and D. Sengupta, Landscape solution to the SUSY flavor and *CP* problems, Phys. Rev. Res. **1**, 033179 (2019).
[97] H. Baer, V. Barger, M. Savoy, and H. Serce, The Higgs mass and natural supersymmetric spectrum from the landscape, Phys. Lett. B **758**, 113 (2016).
[98] H. Baer, V. Barger, and S. Salam, Naturalness versus stringy naturalness (with implications for collider and dark matter searches), Phys. Rev. Res. **1**, 023001 (2019).
[99] H. Baer, V. Barger, J. S. Gainer, P. Huang, M. Savoy, D. Sengupta, and X. Tata, Gluino reach and mass extraction at the LHC in radiatively-driven natural SUSY, Eur. Phys. J. C **77**, 499 (2017).
[100] H. Baer, V. Barger, J. Dutta, D. Sengupta, and K. Zhang, Top squarks from the landscape at high luminosity LHC, Phys. Rev. D **108**, 075027 (2023).
[101] F. E. Paige, S. D. Protopopescu, H. Baer, and X. Tata, ISAJET 7.69: A Monte Carlo event generator for pp, $\bar{p}p$, and $e^{=}e^{-}$ reactions, arXiv:hep-ph/0312045.
[102] W. Beenakker, R. Hopker, and M. Spira, PROSPINO: A program for the production of supersymmetric particles in next-to-leading order QCD, arXiv:hep-ph/9611232.
[103] P. Z. Skands *et al.*, SUSY Les Houches accord: Interfacing SUSY spectrum calculators, decay packages, and event generators, J. High Energy Phys. 07 (2004) 036.
[104] H. Baer and X. Tata, *Weak Scale Supersymmetry: From Superfields to Scattering Events* (Cambridge University Press, Cambridge, England, 2006).
[105] Z. Han, G. D. Kribs, A. Martin, and A. Menon, Hunting quasidegenerate higgsinos, Phys. Rev. D **89**, 075007 (2014).
[106] H. Baer, A. Mustafayev, and X. Tata, Monojet plus soft dilepton signal from light Higgsino pair production at LHC14, Phys. Rev. D **90**, 115007 (2014).
[107] K. J. Bae, H. Baer, V. Barger, and D. Sengupta, Revisiting the SUSY μ problem and its solutions in the LHC era, Phys. Rev. D **99**, 115027 (2019).
[108] H. Baer, V. Barger, N. Nagata, and M. Savoy, Phenomenological profile of top squarks from natural supersymmetry at the LHC, Phys. Rev. D **95**, 055012 (2017); **103**, 059902(E) (2021).
[109] G. Aad *et al.*, Search for supersymmetry in final states with missing transverse momentum and three or more b-jets in 139 fb^{-1} of proton–proton collisions at $\sqrt{s} = 13$ TeV with the ATLAS detector, Eur. Phys. J. C **83**, 561 (2023).
[110] CMS Collaboration *et al.*, Search for supersymmetry in proton-proton collisions at 13 TeV in final states with jets and missing transverse momentum, J. High Energy Phys. 10 (2019) 244.
[111] A. M. Sirunyan *et al.*, Searches for physics beyond the standard model with the M_{T2} variable in hadronic final states with and without disappearing tracks in proton-proton collisions at $\sqrt{s} = 13$ TeV, Eur. Phys. J. C **80**, 3 (2020).
[112] G. Aad *et al.*, Search for charginos and neutralinos in final states with two boosted hadronically decaying bosons and missing transverse momentum in pp collisions at $\sqrt{s} = 13$ TeV with the ATLAS detector, Phys. Rev. D **104**, 112010 (2021).

[113] A. Tumasyan *et al.*, Search for electroweak production of charginos and neutralinos at $s = 13$ TeV in final states containing hadronic decays of WW, WZ, or WH and missing transverse momentum, Phys. Lett. B **842**, 137460 (2023).

[114] S. Kraml, S. Kulkarni, U. Laa, A. Lessa, W. Magerl, D. Proschofsky-Spindler, and W. Waltenberger, SModelS: A tool for interpreting simplified-model results from the LHC and its application to supersymmetry, Eur. Phys. J. C **74**, 2868 (2014).

[115] F. Ambrogi *et al.*, SModelS v1.2: Long-lived particles, combination of signal regions, and other novelties, Comput. Phys. Commun. **251**, 106848 (2020).

[116] G. Alguero, J. Heisig, C. K. Khosa, S. Kraml, S. Kulkarni, A. Lessa, H. Reyes-González, W. Waltenberger, and A. Wongel, Constraining new physics with SModelS version 2, J. High Energy Phys. 08 (2022) 068.

[117] M. Drees, H. Dreiner, D. Schmeier, J. Tattersall, and J. S. Kim, CheckMATE: Confronting your favourite new physics model with LHC data, Comput. Phys. Commun. **187**, 227 (2015).

[118] D. Dercks, N. Desai, J. S. Kim, K. Rolbiecki, J. Tattersall, and T. Weber, CheckMATE2: From the model to the limit, Comput. Phys. Commun. **221**, 383 (2017).

[119] A. M. Sirunyan *et al.*, Search for electroweak production of charginos and neutralinos in multilepton final states in proton-proton collisions at $\sqrt{s} = 13$ TeV, J. High Energy Phys. 03 (2018) 166.

[120] G. Aad *et al.*, Search for squarks and gluinos in final states with jets and missing transverse momentum using 139 fb^{-1} of $\sqrt{s} = 13$ TeV pp collision data with the ATLAS detector. J. High Energy Phys. 02 (2021) 143.

[121] G. Aad *et al.*, Search for chargino–neutralino pair production in final states with three leptons and missing transverse momentum in $\sqrt{s} = 13$ TeV pp collisions with the ATLAS detector, Eur. Phys. J. C **81**, 1118 (2021).

[122] A. Tumasyan *et al.*, Search for supersymmetry in final states with two or three soft leptons and missing transverse momentum in proton-proton collisions at $\sqrt{s} = 13$ TeV, J. High Energy Phys. 04 (2022) 091.

[123] M. Aaboud *et al.*, Search for squarks and gluinos in final states with jets and missing transverse momentum using 36 fb^{-1} of $\sqrt{s} = 13$ TeV pp collision data with the ATLAS detector, Phys. Rev. D **97**, 112001 (2018).

[124] H. Baer, V. Barger, and P. Huang, Hidden SUSY at the LHC: The light Higgsino-world scenario and the role of a lepton collider, J. High Energy Phys. 11 (2011) 031.

[125] H. Baer, V. Barger, S. Salam, D. Sengupta, and X. Tata, The LHC Higgsino discovery plane for present and future SUSY searches, Phys. Lett. B **810**, 135777 (2020).

[126] H. Baer, V. Barger, D. Sengupta, and X. Tata, New angular and other cuts to improve the Higgsino signal at the LHC, Phys. Rev. D **105**, 095017 (2022).

[127] G. Aad *et al.*, Searches for electroweak production of supersymmetric particles with compressed mass spectra in $\sqrt{s} = 13$ TeV pp collisions with the ATLAS detector, Phys. Rev. D **101**, 052005 (2020).

[128] A. Canepa, T. Han, and X. Wang, The search for electroweakinos, Annu. Rev. Nucl. Part. Sci. **70**, 425 (2020).

[129] H. Baer, V. Barger, P. Huang, D. Mickelson, A. Mustafayev, W. Sreethawong, and X. Tata, Same sign diboson signature from supersymmetry models with light Higgsinos at the LHC, Phys. Rev. Lett. **110**, 151801 (2013).

[130] H. Baer, V. Barger, P. Huang, D. Mickelson, A. Mustafayev, W. Sreethawong, and X. Tata, Radiatively-driven natural supersymmetry at the LHC, J. High Energy Phys. 12 (2013) 013; 06 (2015) 53(E).

[131] H. Baer, V. Barger, J. S. Gainer, M. Savoy, D. Sengupta, and X. Tata, Aspects of the same-sign diboson signature from wino pair production with light Higgsinos at the high luminosity LHC, Phys. Rev. D **97**, 035012 (2018).